AIMS Mathematics, 10(10): 23880–23918.
DOI:10.3934/math.20251062
Received: 22 June 2025
Revised: 06 October 2025
Accepted: 11 October 2025
Published: 21 October 2025

https://www.aimspress.com/journal/Math

Research article

Applied statistical modeling of infant mortality with the progressively censored IPMCJ distribution

Mohammad Y. Awajan[1], **Dina A. Ramadan**[1], **Hanan Haj Ahmad**[2,*] **and Beih S. El-Desouky**[1]

[1] Department of Mathematics, Faculty of Science, Mansoura University, Mansoura 33516, Egypt

[2] Department of Mathematics and Statistics, College of Science, King Faisal University, Al-Ahsa 31982, Saudi Arabia

* **Correspondence:** Email: hhajahmed@kfu.edu.sa.

Abstract: Accurate estimation and modeling of infant mortality rates are essential for public health planning and medical research, as they are influenced by a wide range of biological, environmental, and socio-economic factors. To capture the underlying failure patterns, we proposed the inverse power–modified Chris–Jerry (IPMCJ) distribution, a generalized lifetime model particularly suited for decreasing failure rates. Progressive censoring (PC) was incorporated to address the common challenge of incomplete data collection in mortality studies. The statistical properties of the IPMCJ model were studied in detail, and parameter estimation was conducted through maximum likelihood and Bayesian approaches. Bayesian inference was further explored under symmetric squared error and asymmetric linear exponential (LINEX) loss functions, supported by confidence and credible intervals constructed via bootstrap, asymptotic, and Markov chain Monte Carlo (MCMC) methods. The practical relevance of the IPMCJ model was demonstrated using two real infant mortality datasets, where it consistently outperformed ten competing distributions. Convergence was evaluated using maximum likelihood checks and standard Bayesian diagnostics. Model performance of the IPMCJ distribution was validated using (a) the nonparametric Kaplan-Meier estimator and (b) comparisons with the complete-sample analysis. Extensive simulation studies confirmed the robustness and accuracy of the proposed estimators. The results emphasized the value of combining PC with the IPMCJ distribution, offering an effective framework for analyzing infant mortality data and informing health policy decisions.

Keywords: mortality rate; progressive censoring; maximum likelihood estimator; Bayesian estimation; inverse power modified Chris–Jerry distribution; diagnostic tests; Kaplan-Meier; simulation
Mathematics Subject Classification: 62F10, 62F15, 62N01, 62N02, 62N05

1. Introduction

Censoring is a statistical technique that is used to handle incomplete data, particularly in survival analysis and reliability studies. It occurs when the exact value of a data point is unknown due to time constraints, equipment limitations, or other external factors. In clinical research, censoring is crucial, making it essential to develop efficient statistical techniques to overcome these data limitations. Estimating survival functions using specialized methods enables medical practitioners to make informed decisions about patient prognosis and treatment plans. However, if not addressed properly, censoring can distort correlations between variables and potentially lead to misleading conclusions. Furthermore, in industrial reliability tests, censoring helps analyze component failure times, ensuring optimal maintenance strategies.

Various censoring schemes exist, including Type-I, Type-II, progressive, and hybrid censoring, each providing different advantages based on experimental conditions. In Type-I and Type-II censoring schemes, the tests are terminated at a fixed time point T or the $m - th$ failure, respectively. The mixture of these two conventional censoring schemes is termed a hybrid censoring scheme. These methods do not permit the removal of experimental units in intermediate stages. To address this limitation, the progressive censoring (PC) scheme, introduced by Cohen [1], allows the removal of units at different stages of an experiment. Since then, many researchers have analyzed this scheme in various contexts. Balakrishnan and Sandhu [2] proposed algorithms to generate samples from this scheme. For a complete review, one can refer to the books of Balakrishnan and Aggarwala [3] and Balakrishnan and Cramer [4].

Although censoring is essential in data analysis, improper handling can introduce biases. The PC approach has gained attention because of its ability to progressively remove units from tests, making it a cost-effective strategy in lifetime experiments. Researchers have developed different variations of censoring schemes, including optimal censoring schemes, hybrid progressive censoring, and adaptive censoring, each tailored for specific distributions. Kundu [5] explored Bayesian inference under the progressive censoring framework. [6] introduced optimal censoring schemes with the Nadarajah-Haghighi distribution using maximum likelihood estimation (MLE) and Bayesian methods. [7] concentrated on optimal progressive censoring for models characterized by U-shaped hazard rates, applying diverse Bayesian techniques. [8] revisited the progressive Type-I censoring scheme, presenting a historical perspective on its development. [9] also contributed to the field by exploring coherent systems' progressive censoring signature in system reliability applications. Several authors have investigated the PC method under different breakdown scenarios of failure times, see [10] and [11]. In [12], the author examined prediction methods for PC samples, while in [13], the PC scheme was used to investigate the lifetime performance index.

Despite these advancements, efficient models are still needed to flexibly accommodate skewed survival distributions. In response to this, the power Chris–Jerry distribution was introduced by [14] to model skewed lifetime data, incorporating flexible hazard rate structures. Later, [15] proposed an inverse power modified Chris–Jerry (IPMCJ) distribution. The extension IPMCJ provides more flexibility for modeling skewed data and supporting various distributional forms, ranging from nearly symmetric to significantly right-skewed densities.

The rationale for selecting the IPMCJ distribution lies in its ability to model datasets with non-monotonic and heavy-tailed failure behavior. Hence, from a data perspective, the infant mortality

dataset exhibits decreasing hazard rates, which is a typical behavior in early life failure modeling. Traditional distributions such as exponential, Weibull, and even log-normal may not accurately represent such non-monotonic failure patterns.

From a theoretical point of view, the IPMCJ distribution is designed to capture heavy-tailed behavior and bathtub or decreasing hazard functions, which align with the observed characteristics in infant mortality. Moreover, it provides flexibility with its three parameters, and it has hazard shapes that standard models do not.

Therefore, for a fair and interpretable comparison, we focused on distributions commonly used in survival analysis and reliability such as Weibull, Gamma, Log-normal, some generalized C-J distributions and the proposed IPMCJ distribution. These distributions are more aligned with the support and nature of the original complete and censored data.

Additionally, PC is utilized in this study due to its practical advantages in medical and industrial reliability experiments. In such contexts, collecting complete data for every subject is often impractical due to cost, ethical, or time constraints. PC enables partial and efficient data collection while preserving important information about failure mechanisms. This makes it particularly suitable for modeling infant mortality rates, where early failures dominate and study and can be lengthy. A comparative analysis of model fit criteria is performed using complete data and data subjected to a PC scheme. The findings affirm that the IPMCJ distribution not only accommodates censored data effectively but also offers superior model performance under PC, thus supporting its suitability for modeling infant mortality data in settings where progressive censoring is applied.

A nonparametric survival analysis is also incorporated into this study using the Kaplan–Meier (KM) estimator, a well-established method for estimating survival functions under censored data. This analysis provides a reference for assessing the accuracy of the estimate for the proposed parametric model (IPMCJ distribution).

In survival modeling, parameter estimation is essential for drawing valuable conclusions. The MLE, a widely used method for parameter estimation, provides robust estimates under various conditions. However, Bayesian inference methods provide additional advantages, particularly when incorporating prior knowledge about parameters.

This study explores both MLE and Bayesian estimation methods under a PC scheme. The main contributions of this study are as follows:

- Developing a statistical framework for modeling and analyzing infant mortality rates based on the IPMCJ distribution under PC.
- Obtaining point and interval estimates for model parameters and reliability indices, employing MLE and Bayesian approaches.
- Introducing asymptotic confidence intervals and bootstrap methods for parameter estimation.
- Comparing the efficiency of estimation methods using numerical techniques such as Markov Chain Monte Carlo (MCMC).
- Demonstrating the performance of the proposed methodology using real-world infant mortality datasets, by using measures of goodness of fit applied to both censored and complete data.
- Assessing the robustness of the findings via likelihood and Bayesian diagnostics.
- Comparing the parametric IPMCJ with the nonparametric KM estimation method.

The novelty of this study lies not in proposing the IPMCJ distribution itself, but in extending its inferential framework to progressive Type-II censoring schemes, which have not been considered

previously. The present study introduces several methodological and practical enhancements beyond earlier works. First, the proposed model is developed under a progressive censoring framework, increasing its suitability for analyzing incomplete lifetime data. Second, the IPMCJ model's performance is evaluated through a nonparametric comparison with the KM estimator, confirming its flexibility and goodness of fit. Third, both maximum likelihood and Bayesian estimation approaches are established, including asymptotic, bootstrap, and MCMC-based inference. Convergence tests have been evaluated using maximum likelihood checks and standard Bayesian diagnostics to ensure robust parameter estimation. Finally, the proposed methods are validated using two real infant mortality datasets, considering small and large sampled cases, from the World Bank, demonstrating the superior predictive capability of the IPMCJ model compared to several competing lifetime models.

Consequently, the remainder of this study is structured as follows: Section 2 introduces the IPMCJ distribution and the PC sample scheme. Section 3 discusses MLE, while the asymptotic and bootstrap confidence intervals are given in Section 4. Section 5 explores the Bayesian inference under the squared error and linear exponential (LINEX) loss functions with two prior assumptions. Section 6 applies the proposed models to real-world infant mortality datasets, while Section 7 discusses the robustness and validation of the proposed model through the MLE maximum checks and Bayesian diagnostics, as well as comparison with complete data and nonparametric estimators. In Section 8, estimation methods are compared numerically using the MCMC simulations with illustrative tables and figures. Finally, Section 9 concludes the study with key findings and potential directions for future research.

2. Model description

The PC sampling scheme is an effective method that systematically excludes a specific percentage of participants identified as at risk during experiments conducted at various sequential failure intervals. The following demonstrates the PC scheme: In a life-testing experiment, the tester begins with a set of n independent and identically distributed units. The experiment begins with all units under observation and ends with the failure of the $m-th$ unit, where $(m < n)$. When the first failure occurs at time t_1, R_1 units are randomly selected and removed from the remaining $n-1$ surviving units. Similarly, with the second failure at time t_2, the process continues accordingly, and an additional R_2 units are randomly chosen and taken out. leaving $n - R_1 - 2$ surviving units. This process continues, with failure times $(t_3, t_4, ..., t_{m-1})$ being recorded, and corresponding R_i units are removed at each step. The experiment ends with the occurrence of the $m-th$ failure at t_m, at which the number of removed units is determined as: $R_m = n - m - \sum_{i=1}^{m-1} R_i$ and illustrated in Figure 1.

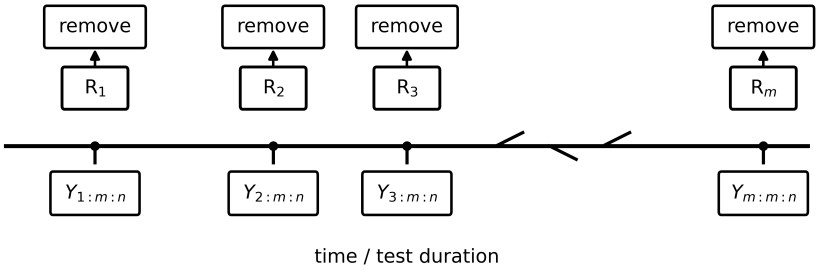

Figure 1. Progressive Type-II censoring scheme.

.

In particular cases, when R_i =0 for i=1, 2, ..., m with $n = m$, the scheme becomes complete sampling, while if $R_i = 0\ for\ i = 1, 2, ..., m-1$, and $R_m = n - m$, it corresponds to the Type-II censoring scheme.

In medical fields, the number of patients in a clinical experiment varies at each stage. With each failure, the pattern of occurrences and observed removals becomes progressively more random. Lifetime distributions such as exponential, log-normal, and Weibull have been the focus of studies on inference for PC, as examined by [16] and [17], that suggested a technique for modeling general PC samples taken from uniform or other continuous distributions. Estimating parameters for different lifetime distributions using PC with certain algorithms have been further explored by [2]. In the context of PC order statistics, [18] examined the D-optimal and A-optimal censoring techniques. [19] determined the parameters of a log-logistic distribution within the context of PC and presented a new spacing-based test statistic to determine whether PC data conforms to an exponential distribution. [20] examined the generalized Rayleigh distribution and its efficiency when applied for modeling data under PC sampling; see [21] and [22].

Many writers have devoted their work to inverted distributions and their uses. In recent years, inverse statistical models have gained increasing attention due to their ability to provide greater flexibility in modeling lifetime and reliability data. Inverse models often exhibit hazard rate shapes that are not easily captured by classical distributions, making them suitable for applications in medical, biological, and engineering sciences. Several inverse extensions of well-known models have been proposed in the literature, such as the inverse Lindley distribution, the inverse Weibull distribution, and the inverse power Lindley distribution, which have demonstrated superior performance in analyzing skewed and heavy-tailed datasets [23–25]. The inversion power Ishita distribution has been studied by [26] under the PC scheme. These inverse models serve as an important motivation for the development of the present study, where we extend the modeling framework to accommodate more complex data patterns and practical applications.

The IPMCJ distribution is a generalization of the modified Chris–Jerry distribution; see [27]. In [15], the model has been demonstrated effectively to capture both infant mortality rates and the fatigue fracture life of Kevlar 373/epoxy composites. The unknown parameters were estimated using the MLE method, and their asymptotic confidence intervals (CIs) were derived based on complete data.

The random variable Y for the IPMCJ distribution has the following probability density function (PDF):

$$f(y;\alpha,\beta,\lambda) = \frac{\alpha\beta^2}{\beta\lambda+2} y^{-\alpha-1}\left(\lambda+\beta y^{-2\alpha}\right)e^{-\beta y^{-\alpha}},\ y>0. \tag{2.1}$$

To ensure that the PDF is valid and integrates to one over the domain $y > 0$, the parameters must satisfy the following conditions, $\alpha > 0, \quad \beta > 0$, and $\lambda > 0$. Additionally, the term $\beta\lambda + 2$ must not be zero. Since $\beta > 0$ and $\lambda > 0$, the denominator is always positive, and the PDF remains well-defined. Figure 2 illustrates the PDF of the IPMCJ distribution under several parameter configurations. As observed, changes in the parameters α, β and λ substantially affect the tail behavior and overall shape of the distribution. For larger values of β and λ, the PDF exhibits heavier tails and slower decay, while smaller α values shift the density toward higher concentration near the origin. This demonstrates the model's flexibility in capturing diverse lifetime data characteristics, including heavy-tailed behaviors often encountered in infant mortality and reliability studies.

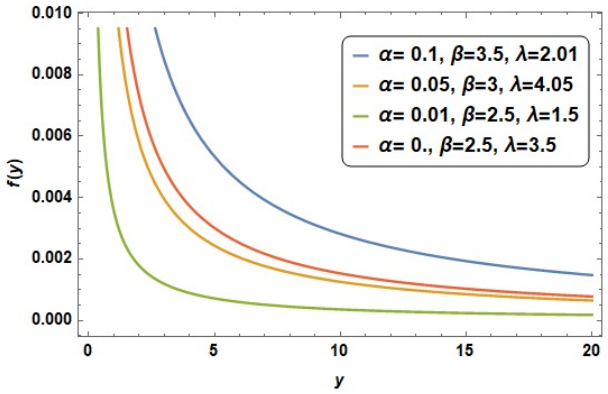

Figure 2. Plot of the pdf of IPMC-J distribution for parameters α, β, and λ.

The cumulative distribution function (CDF) is described as follows:

$$F(y;\alpha,\beta,\lambda) = \frac{\beta y^{-2\alpha} + 2\beta y^{-\alpha} + \beta\lambda + 2}{\beta\lambda + 2} e^{-\beta y^{-\alpha}}, \tag{2.2}$$

where β corresponds to the scale parameter and α, λ correspond to the shape parameters.

The survival function $S(y)$ and the hazard rate function $h(y)$ of the IPMCJ distribution are specified as

$$S(y;\alpha,\beta,\lambda) = 1 - \frac{\beta y^{-2\alpha} + 2\beta y^{-\alpha} + \beta\lambda + 2}{\beta\lambda + 2} e^{-\beta y^{-\alpha}}, \tag{2.3}$$

and

$$h(y;\alpha,\beta,\lambda) = \frac{\alpha\beta^2 y^{-\alpha-1}\left(\lambda + \beta y^{-2\alpha}\right)}{(\beta\lambda + 2)(\beta y^{-2\alpha} + 2\beta y^{-\alpha} + \beta\lambda + 2)}. \tag{2.4}$$

Figure 3 displays the hazard rate function (HRF) of the IPMCJ distribution for different parameter settings. It is evident that the HRF is decreasing in all cases, which reflects a monotonically declining risk over time. Such a pattern is common in reliability and survival data, particularly when the failure rate is higher at the beginning and diminishes with time. The variation in parameter values significantly alters the rate of decline, highlighting the flexibility of the proposed model in capturing different lifetime behaviors.

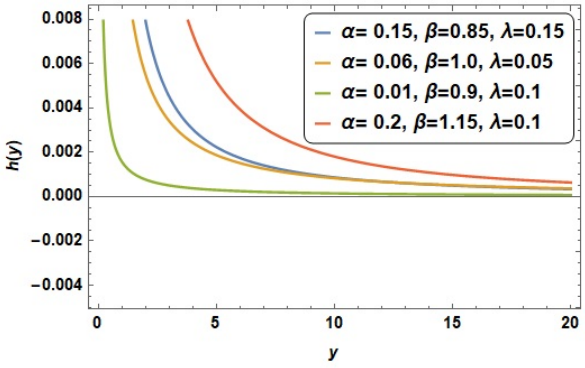

Figure 3. HRF of the of IPMC-J distribution for parameters α, β, and λ.

It is noteworthy that the IPMCJ distribution can be used to depict failure rates exhibiting bathtub and upside-down shapes, as well as datasets with heavy-tailed characteristics, due to its polynomial tail behavior for every value of α, β, and λ, where λ is known as the heavy-tailed parameter. Specifically, as the value of α increases, the upper tail decays more slowly, whereas a decrease in α results in a heavier tail, offering greater flexibility than the modified Chris–Jerry distribution.

The motivation behind developing this new distribution stemmed from the need to analyze life datasets more effectively. Modeling infant mortality requires flexible lifetime distributions capable of capturing the distinctive characteristics of early-life failure patterns, particularly decreasing hazard rates often observed in real-world data. IPMCJ distribution offers an ideal framework due to its adaptability in representing a wide range of distributional shapes, from nearly symmetric to highly right-skewed, and its ability to accommodate monotonic hazard rate structures. These properties make it especially well-suited for infant mortality data, which typically exhibits non-constant risk over time. In practical field studies, collecting complete lifetime data is often constrained by limited resources or ethical considerations. PC presents a realistic and cost-effective solution by allowing partial observation of failure times while maintaining sufficient information for reliable inference. Combining the IPMCJ distribution with PC provides a statistically sound and computationally efficient approach for estimating mortality trends, offering deeper insights for public health decision-making and medical research.

Let $Y_{1;m;n}, Y_{2;m;n}, ..., Y_{m;m;n}$; $1 \leq m \leq n$ represent the results of a PC sample lifetime test conducted with n units, where the data follows an IPMCJ (α, β, λ) distribution and the censoring scheme is defined by $R_1, R_2, ..., R_m$. The joint PDF of the PC scheme is given by:

$$F\left(y_{1;m;n}, y_{2;m:n}, ..., y_{m;m:n}\right) = C \prod_{i=1}^{m} f\left(y_{i;m:n}; \alpha, \beta, \lambda\right)\left[1 - F\left(y_{i;m;n}; \alpha; \beta; \lambda\right)\right]^{R_i}, m < n. \tag{2.5}$$

The constant $C = n(n - R_1 - 1)....(n - \sum_{n=1}^{m-1}(R_i - 1))$ plays a crucial role in defining the likelihood function.

3. Maximum-likelihood estimation

The MLE method is used to tackle the challenge of determining the specifications of the IPMCJ distribution under PC data. Let $y_{1:m:n}, y_{2:m:n}, ..., y_{m:m:n}$ represent a *PC* sample drawn from the IPMCJ distribution with the PDF and CDF given in Eqs (2.1) and (2.2), respectively. Hence, the log-likelihood function is expressed as:

$$\begin{aligned} l(\alpha, \beta, \lambda) \;=\; & m\, ln\, \alpha \; + 2m\, ln\beta \; - m\, ln\left(\beta\lambda + 2\right) \; - (\alpha + 1)\Sigma_{i=1}^{m} ln\, y_i \; + \Sigma_{i=1}^{m} \ln\left(\lambda + \beta y_i^{-2\alpha}\right) \\ & -\beta \sum_{i=1}^{m} y_i^{-\alpha} + \sum_{i=1}^{m} R_i \; \ln\left[1 - \frac{\beta^2 y_i^{-2\alpha} + 2\beta y_i^{-\alpha} + \beta\lambda + 2}{\beta\lambda + 2} e^{-\beta y_i^{-\alpha}}\right]. \end{aligned} \tag{3.1}$$

The MLE of the parameters α, β, and λ are obtained by computing the partial derivatives of the given function Eq (3.1) with respect to α, β, and λ, and setting each derivative to zero will give a system of nonlinear equations:

$$\frac{\partial l}{\partial \alpha} = \frac{m}{\alpha} + \sum_{i=1}^{m}(\beta u_i - 1)\,\ln y_i - 2\sum_{i=1}^{m}\frac{\beta u_i^2\,\ln y_i}{g_i} - \sum_{i=1}^{m}\frac{R_i\,u_i\,\beta^2\,(\beta + \lambda u_i^{-2})\,\ln y_i}{H_i}, \tag{3.2}$$

$$\frac{\partial l}{\partial \beta} = \frac{2m}{\beta} - \frac{m\lambda}{\beta\lambda + 2} - \sum_{i=1}^{m} u_i + \sum_{i=1}^{m}\frac{u_i^2}{g_i} + \sum_{i=1}^{m}\frac{R_i\,\beta\,u_i\left(4\lambda u_i^{-2} + \beta^2\lambda + \beta(2 + \lambda u_i^{-1} + \lambda^2 u_i^{-2})\right)}{(2 + \beta\lambda)\,H_i}, \tag{3.3}$$

and

$$\frac{\partial l}{\partial \lambda} = -\frac{m\beta}{\beta\lambda + 2} + \sum_{i=1}^{m}\frac{1}{g_i} + \sum_{i=1}^{m} R_i\,\frac{\beta^2\,(2u_i^{-1} + \beta u_i^2)}{(2 + \beta\lambda)\,J_i}, \tag{3.4}$$

where

$$u_i = y_i^{-\alpha},$$
$$g_i = \lambda + \beta u_i^2,$$
$$H_i = -2\beta u_i^{-1} - \beta^2 + (e^{\beta u_i} - 1)\,u_i^{-2}(2 + \beta\lambda),$$
$$J_i = -2\beta\,u_i^{-1} + \beta^2 u_i^2 - (2 + \beta\lambda)\,u_i^{-2}(e^{\beta u_i} - 1).$$

Since no closed-form solution exists for the above derivatives, they must be evaluated numerically. Given how challenging it is to solve Eqs. (3.2)–(3.4), nonlinear optimization algorithms like the Newton–Raphson technique are employed. The Newton–Raphson method is a highly effective root-finding algorithm when used appropriately, especially for functions with easily computable derivatives and when a good initial guess is available. However, its limitations necessitate the use of alternative methods to ensure convergence. In this study, the algorithm's convergence is impacted by the careful choice of the parameters' initial values. The logarithmic likelihood surface was numerically checked for monotonicity and unimodality in the region of convergence to ensure that the solution is indeed a global maximum (see Figure 4). In addition, a comprehensive explanation of the algorithm and its implementation is presented in [10]. To ensure reproducibility and clarity, we provide a pseudo-code outline for the numerical implementation of the proposed estimation procedures. For the MLE, the Newton–Raphson algorithm was employed, where initial parameter values are chosen based on method of moments estimates and refined iteratively until convergence. The pseudo-code for the Newton–Raphson algorithm is presented in Appendix B, which facilitates replication of the proposed methods in practice.

Using the MLEs' invariant condition, the MLEs of $S(y)$ and $h(y)$ can be derived by substituting α, β, and λ by $\hat{\alpha}, \hat{\beta}$, and $\hat{\lambda}$ as

$$\hat{S}\left(y; \hat{\alpha}, \hat{\beta}, \hat{\lambda}\right) = 1 - \frac{\hat{\beta}y^{-2\hat{\alpha}} + 2\hat{\beta}y^{-\hat{\alpha}} + \hat{\beta}\hat{\lambda} + 2}{\hat{\beta}\hat{\lambda} + 2}e^{-\hat{\beta}y^{-\hat{\alpha}}}, \tag{3.5}$$

and

$$\hat{h}\left(y; \hat{\alpha}, \hat{\beta}, \hat{\lambda}\right) = \frac{\hat{\alpha}\hat{\beta}^2 y^{-\hat{\alpha}-1}\left(\hat{\lambda} + \hat{\beta}y^{-2\hat{\alpha}}\right)}{(\hat{\beta}\hat{\lambda} + 2)(\hat{\beta}y^{-2\hat{\alpha}} + 2\hat{\beta}y^{-\hat{\alpha}} + \hat{\beta}\hat{\lambda} + 2)}. \tag{3.6}$$

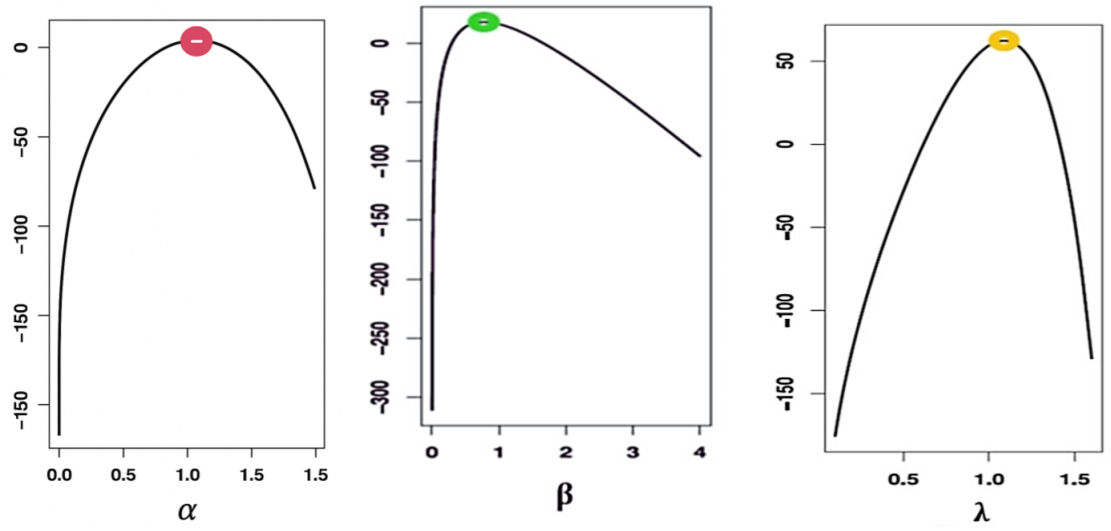

Figure 4. The profile log-likelihood graphs for the parameters α, β, and λ with $m = 10, n = 27$.

4. Confidence intervals

In this section, three different CIs are derived using different techniques.

4.1. Asymptotic CIs

The components of the inverse Fisher information matrix provide an estimate of the variances and covariances of the parameters MLE: $\hat{\alpha}$, $\hat{\beta}$, and $\hat{\lambda}$. The Fisher information matrix is given by: $I_{ij} = \left[-\left[\partial^2 l(\boldsymbol{\eta})/\partial\eta_i\partial\eta_j\right]\right]$, as $i, j = 1, 2, 3$, $\boldsymbol{\eta} = (\eta_1, \eta_2, \eta_3) = (\alpha, \beta, \lambda)$. Due to the complexity of obtaining precise asymptotic forms for these equations, the Fisher information matrix $\hat{I}_{ij}$ is employed to establish the CIs for the parameters through expectation-based inference. Consequently, the observed Fisher information matrix is represented as:

$$\hat{I}_{ij} = \left[\begin{array}{ccc} -\frac{\partial^2 \ln L}{\partial\alpha^2} & -\frac{\partial^2 \ln L}{\partial\alpha\partial\beta} & -\frac{\partial^2 \ln L}{\partial\alpha\partial\lambda} \\ -\frac{\partial^2 \ln L}{\partial\beta\partial\alpha} & -\frac{\partial^2 \ln L}{\partial\beta^2} & -\frac{\partial^2 \ln L}{\partial\beta\partial\lambda} \\ -\frac{\partial^2 \ln L}{\partial\lambda\partial\alpha} & -\frac{\partial^2 \ln L}{\partial\lambda\partial\beta} & -\frac{\partial^2 \ln L}{\partial\lambda^2} \end{array}\right]_{(\alpha=\hat{\alpha},\ \beta=\hat{\beta},\ \lambda=\hat{\lambda})}. \tag{4.1}$$

As a result, the asymptotic variance-covariance matrix V for the MLE is obtained by inverting the observed Fisher information matrix, as follows:

$$\hat{V} = \hat{I}^{-1}_{(\hat{\alpha},\hat{\beta},\hat{\lambda})} = \left[\begin{array}{ccc} var(\hat{\alpha}) & cov(\hat{\alpha},\hat{\beta}) & cov(\hat{\alpha},\hat{\lambda}) \\ cov(\hat{\beta},\hat{\alpha}) & var(\hat{\beta}) & cov(\hat{\beta},\hat{\lambda}) \\ cov(\hat{\lambda},\hat{\alpha}) & cov(\hat{\lambda},\hat{\beta}) & var(\hat{\lambda}) \end{array}\right]. \tag{4.2}$$

The covariance matrix is represented as $I^{-1}(\alpha, \beta, \lambda)$. Consequently, the $(1-\gamma)100\%$ asymptotic confidence intervals (ACIs) for α, β, and λ can be determined as follows:

$$\begin{aligned} &\hat{\alpha} \pm z_{\gamma/2} \sqrt{var\left(\hat{\alpha}\right)}, \\ &\hat{\beta} \pm z_{\gamma/2} \sqrt{var\left(\hat{\beta}\right)}, \\ &\hat{\lambda} \pm z_{\gamma/2} \sqrt{var\left(\hat{\lambda}\right)}, \end{aligned} \tag{4.3}$$

Here, $z_{\gamma/2}$ represents the percentile of the standard normal distribution corresponding to the right-tail probability $\gamma/2$ (see Lawless [28]).

To calculate the ACIs of $S(y)$ and $h(y)$, it depend on the parameters α, β, and λ, respectively. The delta method is applied to approximate the variances of $\hat{S}(y)$ and $\hat{h}(y)$; for more information on the delta method, see Greene [29]. The variance of $\hat{S}(y)$ and $\hat{h}(y)$ can be estimated using this method, respectively.

$$\hat{\sigma}^2_{\hat{S}(y)} = \left[\nabla \hat{S}(y)\right]^T \left[\hat{V}\right] \left[\nabla \hat{S}(y)\right] \text{ and } \hat{\sigma}^2_{\hat{h}(y)} = \left[\nabla \hat{h}(y)\right]^T \left[\hat{V}\right] \left[\nabla \hat{h}(y)\right].$$

The two-sided CIs for $S(y)$ and $h(y)$, which are equal to $100(1-\gamma)\%$, can be formulated as

$$\hat{S}(y) \pm Z_{\frac{\gamma}{2}} \sqrt{\hat{\sigma}^2_{\hat{S}(y)}} \text{and } \hat{h}(y) \pm Z_{\frac{\gamma}{2}} \sqrt{\hat{\sigma}^2_{\hat{h}(y)}}.$$

Due to the nonlinear and complex nature of Eqs. (3.2)–(3.4), closed-form solutions for the parameter estimates are not attainable. As a result, explicit construction of the corresponding CIs is not feasible. Therefore, it becomes necessary to approximate the CIs for the parameters α, β, and λ. To proceed with this approximation, the Fisher information matrix must be derived, which requires calculating the second-order partial derivatives with respect to these parameters. The full explicit forms of the second derivatives remain in Appendix A.

4.2. Bootstrap CIs

This section explores the use of the percentile bootstrap (BOOT-P) and bootstrap-t (BOOT-T) CIs. These intervals produce robust resampling techniques to improve the precision and reliability of parameter estimation methods. For further details on these interval techniques, refer to [30] and [31]. Bootstrap methods provide a resampling-based approach to construct CIs for model parameters and reliability indices. In this study, we employ the percentile bootstrap technique, where resamples of the observed data are generated repeatedly, the parameters are re-estimated for each resample, and the empirical distribution of the estimates is used to form CIs.

In our implementation, the number of bootstrap replications was set to $Nboot = 1000$, a choice widely adopted in the literature to balance estimation accuracy with computational cost. Thus, the bootstrap-based CIs reported in this work are both computationally efficient and statistically reliable.

4.2.1. Parametric bootstrap-P

The parametric percentile BOOT-P formula, used for computing the CIs of the model parameters are derived and expressed as follows:

1) To determine the MLE of α, β, and λ the expressions presented in Eqs (3.2)–(3.4) must be optimized through maximization.

2) Generate BOOT-P samples for α, β, and λ to obtain the estimates Boot-p of α, β, and λ, denoted as η^*,where $\boldsymbol{\eta}$ represents α, β, and λ, from the sample BOOT-P.

3) To obtain $\hat{\eta}_1^*, \hat{\eta}_2^*, ..., \hat{\eta}_{N\ boot}^*$, repeat step 2 for $N\ boot$ iterations, where $\hat{\eta}_i^* = \left(\hat{\alpha}^*, \hat{\beta}^*, \hat{\lambda}^*\right)$,for $i = 1, 2, 3, ..., N\ boot$.

4) Assign $\hat{\eta}_i^*$ for $i = 1, 2, 3, ..., N\ boot$ to $\hat{\eta}_1^*, \hat{\eta}_2^*, ..., \hat{\eta}_{N\ boot}^*$ in ascending order.

$$\left[\hat{\eta}_{N\ boot-p}\left(\frac{\gamma}{2}\right), \hat{\eta}_{N\ boot-p}\left(1-\frac{\gamma}{2}\right)\right], \tag{4.4}$$

which provides a two-sided $100\,(1-\gamma)\,\%$ BOOT-T CIs for the unknown parameters α, β, and λ.

4.2.2. Parametric bootstrap-t

The following steps summarize the BOOT-T CIs algorithm for estimating the model parameters:

1) Follow the same procedure as in the BOOT-P method for Steps 1 and 2 without any modification.

2) Use the asymptotic variance-covariance matrix presented in Eq (4.2), to compute the inverse Fisher information matrix as: $I^{-1}\left(\partial^2 l/\partial\eta_i\partial\eta_j\right);\ i, j = 1, 2, 3$ and calculate the t-statistic of each parameter vector $\boldsymbol{\eta}$ using $T^{*\eta} = (\hat{\eta}^* - \hat{\eta})\,/\,\sqrt{var\,(\hat{\eta}^*)}$.

3) Repeat Steps 3 for each of the N_{boot} bootstrap iterations to obtain the sequence: $T_1^{*\eta}, T_2^{*\eta}, ..., T_{N\ boot}^{*\eta}$.

4) Arrange the resulting t-statistics in ascending order: $T_1^{*\eta} \leq T_2^{*\eta} \leq .... \leq T_{N\ boot}^{*\eta}$.

The two-sided BOOT-T $100\,(1-\gamma)\,\%$ CI for the unknown parameters α, β, and λ are written as

$$\left[\hat{\eta}_{boot-t}\left(\frac{\gamma}{2}\right), \hat{\eta}_{boot-t}\left(1-\frac{\gamma}{2}\right)\right]. \tag{4.5}$$

5. Bayes estimation

For Bayesian estimation of the IPMCJ distribution under PC, it is assumed that α, β, and λ, have the following independent prior gamma $\mathcal{P}_0$ distributions as follows:

$$\begin{aligned} \pi(\alpha) &= \alpha^{a_1-1}e^{-b_1,\alpha}\,, \alpha > 0, \\ \pi(\beta) &= \beta^{a_2-1}e^{-b_2,\beta},\ \beta > 0, \\ \pi(\lambda) &= \lambda^{a_3-1}e^{-b_3,\lambda}\,, \lambda > 0, \end{aligned} \tag{5.1}$$

and another suggested weakly informative prior $\mathcal{P}_{WI}$ as log-normal priors on (α, β, λ):

$$\alpha \sim \text{LogNormal}(\mu_\alpha, \sigma_\alpha^2), \quad \beta \sim \text{LogNormal}(\mu_\beta, \sigma_\beta^2), \quad \lambda \sim \text{LogNormal}(\mu_\lambda, \sigma_\lambda^2).$$

For $x > 0$,

$$\pi_{\text{WI}}(x \mid \mu, \sigma) = \frac{1}{x\,\sigma\,\sqrt{2\pi}}\,\exp\left\{-\frac{(\ln x - \mu)^2}{2\sigma^2}\right\}.$$

As a weakly informative default calibrated on a multiplicative scale, we set $\mu_\alpha = \mu_\beta = \mu_\lambda = 0$ and $\sigma_\alpha = \sigma_\beta = \sigma_\lambda = 1.5$. The weakly informative prior will be used for performing a comparison with the original prior $\mathcal{P}_0$ in Section 6.2. The hyperparameters a_i and b_i, for $i = 1, 2, 3$, are selected to reflect prior beliefs about the unknown parameters and are assumed to be known. In our empirical Bayes

implementation, the hyperparameters are selected using moment-matching based on the observed data. In particular, the prior means are centered at the MLEs, while the prior variances are chosen proportional to the inverse Fisher information. This strategy yields weakly informative priors that are data-driven and reduce subjectivity in the Bayesian inference.

The prior gamma $\mathcal{P}_0$ leads to the formulation of the posterior distribution for the parameters α, β, and λ, which is denoted as: $\pi^*(\alpha,\beta,\lambda \mid y)$.

$$\pi^*(\alpha,\beta,\lambda \mid y) = \frac{\pi(\alpha)\pi(\beta)\pi(\lambda)L(\alpha,\beta,\lambda \mid y)}{\int_0^\infty \int_0^\infty \int_0^\infty \pi(\alpha)\pi(\beta)\pi(\lambda)L(\alpha,\beta,\lambda \mid y)\,d\alpha d\beta d\lambda}. \tag{5.2}$$

To make Bayesian statistical inference more practical and meaningful, it is necessary to consider symmetric and asymmetric loss functions. As noted in [31], a loss function is a real-valued function that accommodates all realistic parameters and estimates. Using such an asymmetric loss function enhances the flexibility and applicability of Bayesian inference in situations where the results of overestimation and underestimation are different. These functions ensure that the inference process remains robust and relevant across various parameter estimators.

Consider the squared error loss (SEL) function , which is defined as

$$L(\eta - \hat{\eta}) = (\eta - \hat{\eta})^2. \tag{5.3}$$

This loss function is symmetric, meaning that it equally penalizes both overestimation and underestimation.

For any function of α, β and λ, the Bayesian estimation $g(\alpha,\beta,\lambda)$ under the SEL function is expressed as:

$$\hat{g}_{BS}(\alpha,\beta,\lambda \mid y) = E_{\alpha,\beta,\lambda|y}(g(\alpha,\beta,\lambda)), \tag{5.4}$$

and

$$E_{\alpha,\beta,\lambda}(g(\alpha,\beta,\lambda)) = \frac{\int_0^\infty \int_0^\infty \int_0^\infty g(\alpha,\beta,\lambda)\pi_1(\alpha)\pi_2(\beta)\pi_3(\lambda)L(\alpha,\beta,\lambda \mid y)\,d\alpha d\beta d\lambda}{\int_0^\infty \int_0^\infty \int_0^\infty \pi_1(\alpha)\pi_2(\beta)\pi_3(\lambda)L(\alpha,\beta,\lambda \mid y)\,d\alpha d\beta d\lambda}. \tag{5.5}$$

The LINEX $L(\triangle)$ for the parameter $\boldsymbol{\eta}$ is defined in [32] and expressed in the following equation:

$$L(\Delta) = \left(e^{\varepsilon\Delta} - \varepsilon\Delta - 1\right), \varepsilon \neq 0, \Delta = \hat{\boldsymbol{\eta}} - \boldsymbol{\eta}. \tag{5.6}$$

Therefore, the Bayesian estimation of a function $g(\alpha,\beta,\lambda)$ under the LINEX is expressed by the following equation:

$$\hat{g}_{\alpha,\beta,\lambda|y} = -\frac{1}{\varepsilon}\log\left[E\left(e^{-\varepsilon\phi(\alpha,\beta,\lambda)} \mid y\right)\right], \varepsilon \neq 0,$$

$$E\left(e^{-g(\alpha,\beta,\lambda)}\right) = \frac{\int_0^\infty \int_0^\infty \int_0^\infty e^{-g(\alpha,\beta,\lambda)}\pi_1(\alpha)\pi_2(\beta)\pi_3(\lambda)L(\alpha,\beta,\lambda \mid y)\,d\alpha d\beta d\lambda}{\int_0^\infty \int_0^\infty \int_0^\infty \pi_1(\alpha)\pi_2(\beta)\pi_3(\lambda)L(\alpha,\beta,\lambda \mid y)\,d\alpha d\beta d\lambda}. \tag{5.7}$$

Noteworthy is the fact that the ratio of several integrals in Eqs (5.5) and (5.7) cannot be clearly stated. Using the joint posterior density function provided to produce samples Eq (5.2), the MCMC

method is employed. Specifically, the MCMC technique is implemented using the Gibbs inside Metropolis–Hastings $(M-H)$ sampling process. The following is the combined posterior distribution:

$$\pi_1^* = \Pi_{i=1}^m \alpha y_i^{-2\alpha} \left(\lambda + \beta y_i^{-2\alpha}\right) e^{-\beta y_i^{-\alpha}} \left[1 - \frac{\beta^2 y_i^{-2\alpha} + 2\beta y_i^{-\alpha} + \beta\lambda + 2}{\beta\lambda + 2} e^{-\beta y_i^{-\alpha}}\right]^{R_i}, \tag{5.8}$$

$$\pi_2^* = \Pi_{i=1}^m \frac{\beta^2}{\beta\lambda + 2} \left(\lambda + \beta y_i^{-2\alpha}\right) e^{-\beta y_i^{-\alpha}} \left[1 - \frac{\beta^2 y_i^{-2\alpha} + 2\beta y_i^{-\alpha} + \beta\lambda + 2}{\beta\lambda + 2} e^{-\beta y_i^{-\alpha}}\right]^{R_i} \tag{5.9}$$

and

$$\pi_3^* = \Pi_{i=1}^m \frac{1}{\beta\lambda + 2} \left(\lambda + \beta y_i^{-2\alpha}\right) e^{-\beta y_i^{-\alpha}} \left[1 - \frac{\beta^2 y_i^{-2\alpha} + 2\beta y_i^{-\alpha} + \beta\lambda + 2}{\beta\lambda + 2} e^{-\beta y_i^{-\alpha}}\right]^{R_i}. \tag{5.10}$$

The Bayesian estimation of the parameters α, β and λ for the IPMCJ distribution is analytically intractable due to the model's complexity. Closed-form solutions are difficult to obtain under the conditions of the IPMCJ distribution. To overcome this challenge, we propose the use of the MCMC method, a robust computational approach for estimating posterior distributions when analytical solutions are unavailable; see Eq (5.2).

It is evident from Eqs (5.8)–(5.10) that the conditional posterior distributions of α, β and λ do not correspond to any standard form. As a result, Gibbs sampling becomes an appropriate choice, where the M–H algorithm plays a crucial role in drawing samples within the MCMC framework. The MCMC method generates a sequence of samples that approximate the posterior distribution of the model parameters by simulating a Markov chain that converges to the target distribution. These samples can be used to estimate posterior statistics, such as the mean, which serves as Bayesian estimation for α, β, and λ. In the Bayesian framework, the M–H sampler was implemented to generate posterior samples, with acceptance probabilities defined by the ratio of likelihood and prior terms. The pseudo-code for the M–H algorithm is presented in Appendix C, which facilitates replication of the proposed methods in practice.

Gibbs sampling is especially effective when conditional sampling of each parameter, given the others, is feasible, see Metropolis et al. [33] and Hastings [34]. During each iteration, the parameters are updated sequentially by sampling from their respective conditional distributions, thereby enabling efficient exploration of the parameter space. For further details regarding the algorithm's structure, one can refer to [35]. Since the full conditional distributions do not match any known standard forms, the M–H algorithm is employed within the Gibbs sampling framework, as seen in [36].

We now describe the steps of the M–H within the Gibbs sampling procedure used to generate posterior samples:

1) Start with the initial values $(\alpha^{(0)}, \beta^{(0)}, \lambda^{(0)})$,

2) Set the iteration index j =1.

3) Proposal Generation: (i) Generate proposals $\alpha^*, \beta^*, \lambda^*$ from normal distributions as follows: $\alpha^* \sim N\left(\alpha^{(j-1)}, var(\alpha)\right)$, $\beta^* \sim N\left(\beta^{(j-1)}, var(\beta)\right)$, $\lambda^* \sim N\left(\lambda^{(j-1)}, var(\lambda)\right)$ are suggestion to α^*, β^*, and λ^*. Here, $var(.)$ represents the variance that can be obtained from the diagonal elements of the inverse of the observed Fisher information matrix.

4) Compute the acceptance probabilities

$$\rho_\alpha = \min\left[1, \frac{\pi_1^*\left(\alpha^* \mid \beta^{(j-1)}, \lambda^{(j-1)}, y\right)}{\pi_1^*\left(\alpha^{j-1} \mid \beta^{(j-1)}, \lambda^{(j-1)}, y\right)}\right], \tag{5.11}$$

$$\rho_\beta = \min\left[1, \frac{\pi_1^*\left(\beta^* \mid \alpha^{(j-1)}, \lambda^{(j-1)}, y\right)}{\pi_1^*\left(\beta^{(j-1)} \mid \alpha^{(j-1)}, \lambda^{(j-1)}, y\right)}\right] \tag{5.12}$$

and

$$\rho_\lambda = \min\left[1, \frac{\pi_2^*\left(\lambda^* \mid \alpha^{(j-1)}, \beta^{(j-1)}, y\right)}{\pi_2^*\left(\lambda^{(j-1)} \mid \alpha^{(j-1)}, \beta^{(j-1)}, y\right)}\right]. \tag{5.13}$$

5) Acceptance and rejection (i) Generate u_1, u_2, and u_3 from a uniform distribution $U(0, 1)$

(ii) If $u_1 < \rho_\alpha$, accept the proposition and set $\alpha^{(j)} = \alpha^*$; otherwise, set $\alpha^{(j)} = \alpha^{(j-1)}$.

(iii) If $u_2 < \rho_\beta$, accept the proposition and set $\beta^{(j)} = \beta^*$; otherwise, set $\beta^{(j)} = \beta^{(j-1)}$.

(iv) If $u_3 < \rho_\lambda$, accept the proposition and set $\lambda^{(j)} = \lambda^*$; or else, specify $\lambda^{(j)} = \lambda^{(j-1)}$.

6) Set $j = j + 1$ and repeat steps 3–6 for N iterations.

7) After sufficient iterations, posterior means of α^j, β^j, and λ^j are used as Bayesian estimates.

8) To construct the credible intervals (CRI) for α, β, and λ,

(i) let $\eta_k^{(i)}, i = 1, 2, ..., N, k = 1, 2, 3$ represent the ordered samples for $(\eta_1, \eta_2, \eta_3) = (\alpha, \beta, \lambda)$ such that $\eta_k^{(1)} < \eta_k^{(2)} < \cdots < \eta_k^{(N)}$.

(ii) The $(1 - \gamma)\,100\%$ CRI for η_k is derived using the appropriate quantiles from the ordered posterior samples as:

$$\left(\eta_k(\frac{\gamma}{2}(N - M)), \eta_k((1 - \frac{\gamma}{2})(N - M))\right). \tag{5.14}$$

For a sufficiently large N , the selected samples are $\eta_k^{(j)}, j = M + 1, ..., N$. The SEL function is used to obtain the approximate Bayesian estimation of α, β, and λ as follows:

$$\hat{\alpha}_{BS} = \frac{1}{N - M}\sum_{j=M+1}^{N} \alpha^{(j)}, \tag{5.15}$$

$$\hat{\beta}_{BS} = \frac{1}{N - M}\sum_{j=M+1}^{N} \beta^{(j)} \tag{5.16}$$

and

$$\hat{\lambda}_{BS} = \frac{1}{N - M}\sum_{j=M+1}^{N} \lambda^{(j)}. \tag{5.17}$$

The parameter estimates under LINEX are provided as follows:

$$\hat{\alpha}_{BL} = \frac{-1}{c}\log\left[\frac{1}{N - M}\sum_{j=M+1}^{N} e^{-c\alpha^{(i)}}\right], \tag{5.18}$$

$$\hat{\beta}_{BL} = \frac{-1}{c} \log \left[\frac{1}{N-M} \sum_{j=M+1}^{N} e^{-c\beta^{(i)}} \right] \tag{5.19}$$

and

$$\hat{\lambda}_{BL} = \frac{-1}{c} \log \left[\frac{1}{N-M} \sum_{j=M+1}^{N} e^{-c\lambda^{(i)}} \right]. \tag{5.20}$$

6. Real-life data applications

In this section, we apply the statistical techniques introduced in the preceding sections to achieve the analysis objectives and highlight the significance of statistical inference as a fundamental tool. *Wolfram Mathematica 13.0* software was used to perform numerical techniques.

The analysis is carried out using the data on the infant mortality rate to facilitate data interpretation and improve the performance and efficiency of the IPMCJ model under PC. We consider two datasets that include the infant mortality rate per 1,000 live births for a selection of countries as reported by the World Bank (`https://data.worldbank.org/indicator/SP.DYN.IMRT.IN`). The two examples have been chosen on the basis of small and large sample sizes to enhance the practical application of the proposed model.

To assess the efficiency of the IPMCJ distribution in modeling the infant mortality rate compared to other competing distributions, we contrast the goodness of fit tests of the IPMCJ with the following distributions: Exponentiated Weibull (Exp Weibull) [37], Extended Weibull (Ext Weibull) [38], Gamma Weibull [39], Exponentiated Inverse Exponential (EIE) distribution [40], modified Weibull distribution [41], Burr III distribution by [42], Gamma distribution [43], the Chris–Jerry (C–J) distribution by [44], two-parameter Chris-Jerry (TPCJ) distribution by [45], and Lomax distribution [46], based on PC sample.

For model comparison, we employ several goodness-of-fit measures: the negative log-likelihood ($-L$), Akaike information criterion (AIC), Bayesian information criterion (BIC), corrected AIC (CAIC), Shapiro-Wilk statistic (W^*), Anderson-Darling statistic (A^*), and the Kolmogorov–Smirnov test (K-S) with the corresponding p-value.

6.1. Mortality rate 2021 (Small sample size)

Infant mortality rates have been observed from different countries in 2021. A PC sample consisting of $m = 10$ elements was randomly selected from a dataset of size $n = 27$, following the censoring scheme $(7, 6, 0, 0, 0, 0, 0, 0, 0, 0)$. The failure times and censoring counts are explored in Table 1.

In Table 2, the estimation of the parameters is evaluated for different distributions, which provides an assessment of the fitness of IPMCJ to the infant mortality data.

The goodness-of-fit tests have been performed for the above mortality rate, and the results are summarized in Table 3. It is observed that the IPMCJ distribution achieves the lowest values for all information criteria and the highest K–S (p-value) among the candidate models. Therefore, we conclude that the IPMCJ distribution provides the best overall fit to the infant mortality data.

The MLE estimation of the parameters α, β, and λ, are derived from the PC failure data in Table 1, and presented in Table 2. The BOOT-P and BOOT-T samples were obtained following the procedure outlined in Section 4 of the bootstrap methods. Bayesian estimation is performed using SEL and LINEX loss functions, where the latter is analyzed using different values of the shape parameter c, $c = \{-2, 0.0001, 2\}$.

Table 1. Progressive Type-II censoring scheme for $m = 10, n = 27$: mortality rate failure times X_i and censoring counts R_i.

x_i	56	10	22	3	69	6	7	11	4
R_i	7	6	0	0	0	0	0	0	0
x_i	4	19	13	7	27	12	3	4	11
R_i	0	0	0	0	0	0	0	0	0
x_i	84	27	25	6	35	14	11	12	6
R_i	0	0	0	0	0	0	0	0	0

Table 2. Estimates of parameters for the distributions fitted to infant mortality data (PC scheme).

Model	α	β	λ
Three-parameter models			
IPMC–J(α, β, λ)	0.73	0.031	0.54
Exp Weibull(α, β, λ)	0.066	1.125	0.821
Ext Weibull(α, β, λ)	1.813	3.026	1.959
Gamma Weibull(α, β, λ)	0.111	1.209	9.202
Two- and one-parameter models			
TPCJ(β, λ)	–	3.25	0.16
Burr III(β, λ)	–	5.40	0.03
EIE(β, λ)	–	0.25	5.66
Weibull(β, λ)	–	0.82	5.70
Gamma(β, λ)	–	0.80	7.42
Lomax(β, λ)	–	32.11	8.74
C–J(β)	–	0.40	–

Table 3. Model selection under PC.

Model	$-L$	AIC	BIC	CAIC	W^*	A^*	K–S	p-value
Three-parameter models								
IPMCJ(α, β, λ)	99.66	201.33	201.62	201.49	0.037	0.20	0.040	0.645
Exp Weibull(α, β, λ)	109.10	203.40	203.60	202.10	0.045	0.25	0.131	0.568
Ext Weibull(α, β, λ)	102.50	204.51	204.80	201.20	0.057	0.35	0.174	0.581
Gamma Weibull(α, β, λ)	103.10	215.40	214.91	205.30	0.069	0.42	0.245	0.180
Two- and one-parameter models								
TPCJ(β, λ)	100.16	216.31	205.90	210.81	0.12	0.54	0.15	0.645
Burr III(β, λ)	110.08	220.16	220.75	222.66	0.05	0.22	0.26	0.021
EIE(β, λ)	101.88	209.76	206.36	209.26	0.07	0.40	0.15	0.207
Weibull(β, λ)	102.11	225.36	213.95	221.86	0.14	0.62	0.22	0.084
Gamma(β, λ)	105.76	207.90	210.49	208.40	0.17	0.42	0.17	0.436
Lomax(β, λ)	104.17	206.33	208.92	211.83	0.21	0.61	0.15	0.581
C–J(β)	109.39	226.77	205.07	216.93	0.16	1.23	0.34	0.260

Table 4 indicates that all estimation methods produce nearly identical point estimates for the IPMCJ parameters and the two reliability measures, indicating strong agreement across frequentist and Bayesian approaches. The shape parameter α ranges around 0.67–0.74, the scale parameter β around 0.03–0.08, and the location parameter λ around 0.54–0.59. Consequently, the estimated survival probability at $t = 0.5$ remains high (0.82) and the instantaneous hazard rate moderate (0.40), regardless of method. This consistency demonstrates the robustness of the IPMCJ model's inference for infant mortality data under both bootstrap and Bayesian estimation schemes. In Table 4, the results of the SEL and LINEX loss functions are identical at $c = 0.0001$, which confirms the accuracy of the presented estimates.

Table 4. Point estimation of the model parameters, $h(t)$, and $S(t)$ with mean square error (MSE) for the infant mortality rate data.

Parameter	Frequentist Estimates			Bayesian Estimates			
	MLE	BOOT-P	BOOT-T	SEL	LINEX (c)		
					-2	0.0001	2
α	0.7392	0.6987	0.6994	0.6749	0.6776	0.6723	0.6749
	(0.00617)	(0.00896)	(0.00675)	(0.00692)	(0.00732)	(0.00707)	(0.00921)
β	0.0326	0.0645	0.0554	0.0746	0.0747	0.0745	0.0746
	(0.0094)	(0.01017)	(0.00952)	(0.01032)	(0.00257)	(0.03498)	(0.04505)
λ	0.5407	0.5901	0.5784	0.5735	0.5834	0.5636	0.5735
	(0.03401)	(0.05054)	(0.03943)	(0.06463)	(0.05567)	(0.04527)	(0.05764)
$S(0.5)$	0.8193	0.8452	0.8341	0.8224	0.8229	0.8219	0.8224
	(0.00274)	(0.00319)	(0.00362)	(0.00288)	(0.00290)	(0.00364)	(0.00441)
$h(0.5)$	0.3975	0.3994	0.3987	0.3983	0.4009	0.3958	0.3983
	(0.00305)	(0.00477)	(0.00532)	(0.00568)	(0.0072)	(0.0077)	(0.00937)

In Table 5, the average confidence length (ACL) and the coverage probability (CP) are calculated for a 95% ACI, BOOT-P, BOOT-T, and CRI. The probability of coverage refers to the percentage of times that the interval captures the actual value of the parameter of interest.

The combination of these methods demonstrates the consistency and robustness of model parameter estimation. The parameter estimates appear to be reliable, and the uncertainty is quantified in a variety of ways. It is important to note that while the MLE and bootstrap methods produce wide CIs that include negative values or zeros for parameters that must be strictly positive, the MCMC-based Bayesian credible intervals remained within the theoretical parameter space. This indicates that Bayesian estimation under the IPMCJ model provides more reliable and statistically significant parameter estimates, especially in the presence of PC. This behavior highlights the limitations of classical estimation methods under PC for small or skewed samples, especially when the likelihood surface is flat or irregular.

Table 5. 95% CIs with ACL and (CP) for ACI, BOOT-P, BOOT-T and CRI for model parameters, $S(t)$ and $h(t)$ for infant mortality rate data with $m = 10, n = 27$.

Parameter	ACI	BOOT-P	BOOT-T	MCMC
α	0.6490 (0.9280)	0.5367 (0.8540)	0.5914 (0.9170)	0.6420 (0.9220)
β	0.4920 (0.9530)	0.4208 (0.8500)	0.4611 (0.9320)	0.4966 (0.9500)
λ	0.4174 (0.8420)	0.4521 (0.9300)	0.3498 (0.9470)	0.2823 (0.7850)
$S(0.5)$	0.7095 (0.9410)	0.6088 (0.8520)	0.6638 (0.9350)	0.6656 (0.9300)
$h(0.5)$	0.3592 (0.9510)	0.3064 (0.8600)	0.3296 (0.9410)	0.3416 (0.8880)

6.2. Mortality rate 2023 (Large sample size)

Infant mortality rates have been observed in different countries in 2023. A PC sample consisting of $m = 70$ elements was randomly selected from a dataset of size $n = 244$, following a censoring scheme that is shown in Table 6.

The MLE estimation of the parameters α, β and λ, are derived from the PC failure data in Table 6, and presented in Table 7.

The goodness-of-fit tests have been performed and the results are summarized in Table 8. It is observed that the IPMCJ distribution achieves the lowest values for almost all information criteria with the highest K–S (p-value) among other candidate models. Therefore, we conclude that the IPMCJ distribution provides the best overall fit to the infant mortality data with a large sample size.

The BOOT-P and BOOT-T samples can be obtained in a similar way as mentioned in Section 6.1, and following the procedure outlined in Section 4 of the bootstrap methods. Bayesian estimation can be performed using SEL and LINEX loss functions using different values of the shape parameter c.

Table 6. Progressive Type-II censoring scheme for $m = 70, n = 244$: mortality rate failure times X_i and censoring counts R_i.

i	X_i	R_i	i	X_i	R_i	i	X_i	R_i	i	X_i	R_i	i	X_i	R_i
1	1.4	32	15	2.1	3	29	2.6	1	43	3.0	0	57	3.3	0
2	1.6	26	16	2.2	3	30	2.6	1	44	3.0	0	58	3.3	0
3	1.7	22	17	2.2	3	31	2.7	1	45	3.0	0	59	3.3	0
4	1.8	18	18	2.2	3	32	2.7	0	46	3.1	0	60	3.4	0
5	1.8	15	19	2.2	2	33	2.7	0	47	3.1	0	61	3.4	0
6	1.8	12	20	2.3	2	34	2.8	0	48	3.1	0	62	3.5	0
7	1.9	10	21	2.3	2	35	2.8	0	49	3.1	0	63	3.5	0
8	1.9	8	22	2.3	2	36	2.8	0	50	3.1	0	64	3.5	0
9	1.9	7	23	2.3	2	37	2.9	0	51	3.1	0	65	3.5	0
10	2.0	6	24	2.3	1	38	2.9	0	52	3.2	0	66	3.5	0
11	2.0	5	25	2.4	1	39	2.9	0	53	3.2	0	67	3.5	0
12	2.1	4	26	2.4	1	40	3.0	0	54	3.2	0	68	3.7	0
13	2.1	4	27	2.5	1	41	3.0	0	55	3.2	0	69	3.8	0
14	2.1	3	28	2.5	1	42	3.0	0	56	3.2	0	70	7.571	0

Table 7. Estimates of parameters for the distributions fitted to the progressive Type-II censored data ($m = 70$).

Model	α	β	λ
Three-parameter models			
IPMCJ(α, β, λ)	2.734	23.113	0.773
Exp Weibull(α, β, λ)	1.344	8.721	0.452
Ext Weibull(α, β, λ)	1.781	10.441	1.231
Gamma Weibull(α, β, λ)	0.987	14.251	2.451
Two-parameter models			
TPCJ(β, λ)	–	2.130	1.542
Burr III(β, λ)	–	3.016	2.329
EIE(β, λ)	–	2.740	1.891
Weibull(α, λ)	3.186	–	4.584
Gamma(β, λ)	–	2.312	1.985
Lomax(β, λ)	–	3.441	2.782
C–J(β)	–	4.560	–

Table 8. Model selection under PC ($m = 70$).

Model	$-L$	AIC	BIC	CAIC	W^*	A^*	K–S	p-value
Three-parameter models								
IPMCJ(α, β, λ)	135.59	277.17	283.92	277.54	0.108	95.84	0.101	0.444
Exp Weibull(α, β, λ)	155.12	295.22	301.44	299.01	0.241	50.221	0.210	0.391
Ext Weibull(α, β, λ)	148.21	289.21	299.45	312.11	0.212	66.651	0.140	0.334
Gamma Weibull(α, β, λ)	166.21	311.01	298.11	288.10	0.311	70.660	0.224	0.401
Two-parameter models								
TPCJ(β, λ)	144.23	288.23	291.10	288.41	0.223	85.41	0.341	0.244
Burr III(β, λ)	134.91	275.82	282.56	276.18	0.161	95.05	0.115	0.286
EIE(β, λ)	150.22	299.33	310.22	294.11	0.516	88.21	0.311	0.112
Weibull(α, λ)	139.64	283.28	287.78	283.46	0.785	85.51	0.199	0.007
Gamma(β, λ)	139.99	320.01	298.22	297.45	0.812	80.55	0.284	0.281
Lomax(β, λ)	145.22	279.56	288.58	301.55	0.245	90.24	0.381	0.304
C–J(β)	144.55	301.22	286.42	299.34	0.712	65.32	0.271	0.400

7. Robustness and validation

We now assess robustness of the findings via the PC dataset (2021), a complete-data comparison, likelihood and Bayesian diagnostics, and a nonparametric benchmark.

7.1. MLE maximum-checks

Consider the log-likelihood function for IPMCJ as given in Eq (3.1). Let $\hat{\boldsymbol{\eta}} = (\hat{\alpha}, \hat{\beta}, \hat{\lambda})$ be the MLE. To verify that $\hat{\boldsymbol{\eta}}$ corresponds to an exact maximum, we report three complementary diagnostics. These diagnostics are checked for the first mortality rate dataset with $m = 10, n = 27$.

(a) Observed Hessian at the MLE. We approximate the observed Hessian

$$H(\hat{\boldsymbol{\eta}}) \;=\; \partial^2 l(\boldsymbol{\eta}) / \partial\eta_i \partial\eta_j, i = j = 1, 2, 3.$$

The eigenvalues $(\zeta_{(1)}, \zeta_{(2)}, \zeta_{(3)})$ of $H(\hat{\boldsymbol{\eta}})$ are all negative (see Table 9) confirming a negative definite matrix. Equivalently, the observed information $I(\hat{\boldsymbol{\eta}}) = -H(\hat{\boldsymbol{\eta}})$ is positive definite. Hessian has been computed via central differences in log parameters. Reported eigenvalues are of negative signs, and the final log-likelihood value is obtained to be -112.6210 for a different initial value of the parameters as reported in Table 10.

(b) Multi-start optimization: To protect against dependence on initialization, we optimize in $\boldsymbol{\theta} = \log \boldsymbol{\eta}$. Each run uses the same method and stopping rules. All runs converge to the same $\hat{\boldsymbol{\eta}}$ (to within 10^{-6} in parameters) and to the same $\ell(\hat{\boldsymbol{\eta}})$ (to within 10^{-6}), as summarized in Table 10.

(c) Profile and surface-based likelihood diagnostics: For each parameter, we compute the profile likelihood as displayed in Figure 4.

In all the above cases, we observe a single, well-defined basin centered at the MLEs, providing visual evidence against secondary local maxima.

Optimization is conducted in the log-parameter space using a quasi-Newton method with gradient tolerance 10^{-8} and step tolerance 10^{-8}. Numerical derivatives use central differences with step 10^{-4}; we verified stability under a factor of 10 perturbation of this step. All randomization (for multi-starts) uses a fixed seed, reported in Table 10.

Table 9. Observed Hessian eigenvalues at the MLE $(\hat{\alpha}, \hat{\beta}, \hat{\lambda})$. Negative eigenvalues confirm a strict local maximum.

Dataset	$\hat{\alpha}$	$\hat{\beta}$	$\hat{\lambda}$	$\zeta_{(1)}$	$\zeta_{(2)}$	$\zeta_{(3)}$
Main	0.5497	12.1140	6.40568821e-09	-284.4071	-18.2442	$-3.55271327e-07$

Table 10. Multi-start optimization summary (performed in log-parameter space). All runs converge to the same MLE and final log-likelihood (tolerance $< 10^{-6}$).

Run	$(\alpha_0, \beta_0, \lambda_0)$	$\hat{\alpha}$ (MLE)	$\hat{\beta}$ (MLE)	$\hat{\lambda}$ (MLE)	Final log-likelihood	iterations	Status
1	(1.00, 1.00, 1.00)	0.549643	12.112760	1.662×10^{-8}	-112.621035	38	converge
2	(1.50, 0.90, 0.60)	0.549642	12.112720	1.002×10^{-9}	-112.621034	40	converge
3	(0.50, 5.00, 2.00)	0.549655	12.113310	4.237×10^{-9}	-112.621034	40	converge
4	(0.85, 2.00, 0.01)	0.549644	12.112700	2.558×10^{-8}	-112.621035	32	converge

7.2. Bayesian diagnostics

We fit the Bayesian model using $C = 4$ parallel chains with S post-warmup draws per chain. Convergence and mixing are assessed with standard scalar and graphical diagnostics. Here are the three diagnostic tests that we conduct to demonstrate convergence in Bayesian inference using the dataset $m = 10, n = 27$. A similar argument can be applied to the second dataset, with $m = 70$ and $n = 244$.

(a) Convergence diagnostics: For each parameter we compute split $\hat{R}$ and effective sample sizes $\mathrm{ESS}_{\mathrm{bulk}}$ and $\mathrm{ESS}_{\mathrm{tail}}$. Table 11 reports numerical summaries together with posterior means and 95% credible intervals. Split-$\hat{R}$ near 1.00 and large ESS indicate good mixing and convergence. $\mathrm{ESS}_{\mathrm{bulk}}$ targets central behavior; $\mathrm{ESS}_{\mathrm{tail}}$ targets tail behavior. Figure 5 displays autocorrelation functions that decay rapidly within each chain.

(b) Acceptance and sampler rate: Table 12 reports acceptance rates per chain and the overall effective draws under the prior $\mathcal{P}_0$. We also inspected the empirical autocorrelations and between-chain variances; no chain exhibited pathological behavior.

(c) Prior sensitivity: To assess robustness, we re-estimated the posterior under the weakly informative prior $\mathcal{P}_{\mathrm{WI}}$, contrasted with our originally specified Gamma prior $\mathcal{P}_0$. Table 13 compares posterior means and 95% credible intervals under $\mathcal{P}_0$ vs. $\mathcal{P}_{\mathrm{WI}}$, along with the absolute relative difference (ARD) in posterior means. Figure 6 overlays marginal posteriors under the two priors. Across parameters, differences are negligible to small and do not alter substantive conclusions. We use a common random seed across runs, identical sampler settings across chains, and retain all post-warmup draws for diagnostics.

Table 11. Posterior summaries and convergence diagnostics (P0).

Param	Mean	95% CrI Low	95% CrI High	R-hat	ESS(bulk)	ESS(tail)
α	0.8749	0.6715	1.105	1.045	75	109
β	9.9650	5.9150	15.080	1.033	38	58
λ	3.9940	0.4700	13.550	1.300	12	16

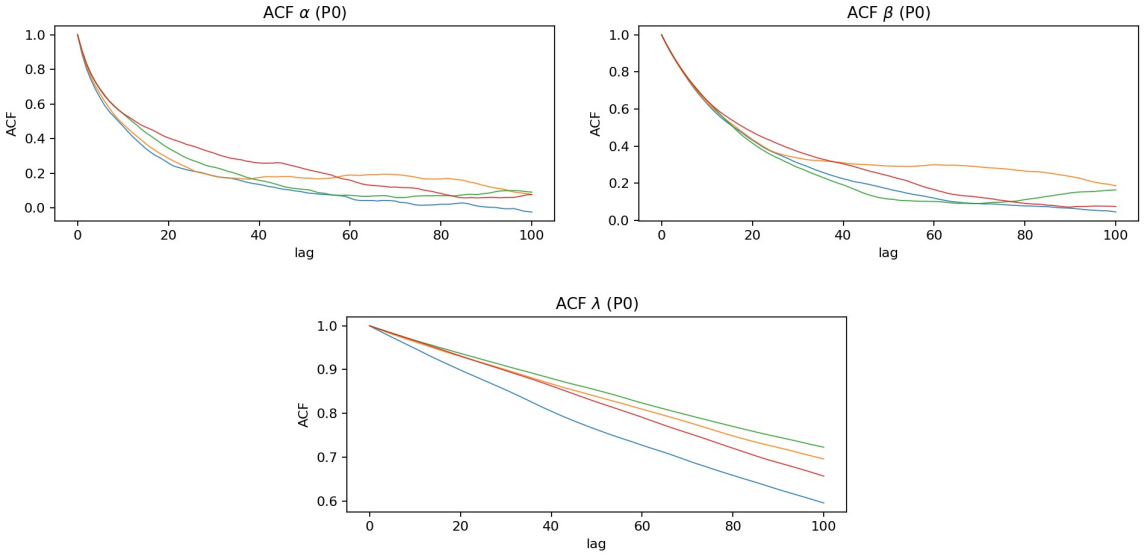

Figure 5. Within-chain autocorrelation functions showing rapid decay, consistent with adequate effective information.

Table 12. Chain-level diagnostics for prior $\mathcal{P}_0$.

Chain	Acceptance rate	Avg. lag-1 ACF	Effective draws (overall)
1	0.455	0.909	79
2	0.467	0.938	52
3	0.463	0.931	40
4	0.458	0.941	42

Table 13. Prior sensitivity: posterior summaries under the originally specified prior $\mathcal{P}0$ versus a weakly-informative prior $\mathcal{P}$WI.

	$\mathcal{P}0$		$\mathcal{P}$WI		ARD (%) $\frac{\lvert\text{Mean}_{\text{WI}}-\text{Mean}_0\rvert}{\lvert\text{Mean}_0\rvert}\times 100$
Parameter	Mean	95% CrI	Mean	95% CrI	
α	0.8749	[0.6715, 1.105]	0.9381	[0.6978, 1.254]	7.22
β	9.9650	[5.9150, 15.08]	10.99	[5.577, 20.74]	10.29
λ	3.9940	[0.4700, 13.55]	25.45	[2.412, 73.06]	537.2

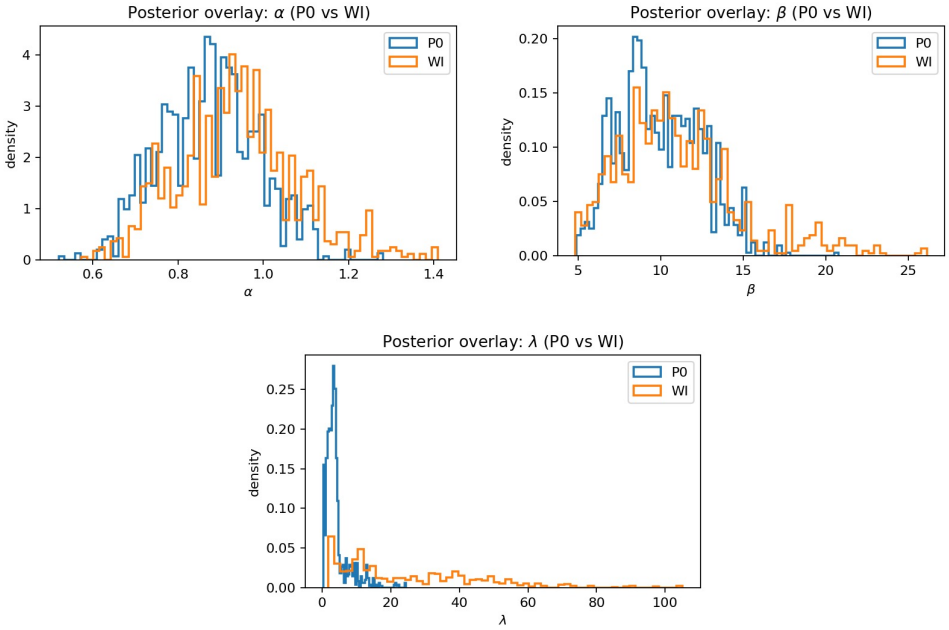

Figure 6. Prior sensitivity: marginal posterior densities under the originally specified prior $\mathcal{P}_0$ and a weakly-informative prior $\mathcal{P}_{WI}$.

From the above tables and graphs, we can summarize the main results as:

- Random walk Metropolis acceptance rates are ≈ 0.44-0.47 for both priors. which is on the high side for 3D targets (typical target ~0.20–0.35). This suggests the proposal step size is somewhat conservative, which can increase autocorrelation.
- Convergence with $\hat{R}$ under $\mathcal{P}_0$, $\hat{R}$ is acceptable/borderline for (α,β) (1.045, 1.033) but unsatisfactory for λ (1.300). Under $\mathcal{P}_{\mathrm{WI}}$, all $\hat{R}$ values worsen, especially λ (1.891). Target is $\hat{R} \leq 1.01$–1.05.
- Effective sample sizes: $\mathrm{ESS}_{\mathrm{bulk}}$ for λ is low (12 under $\mathcal{P}_0$, 21 under $\mathcal{P}_{\mathrm{WI}}$), with modest tail ESS. This indicates strong autocorrelation and poor mixing for λ; (α,β) are also modest.
- Prior sensitivity: Posterior means and 95% CrIs for α and β shift moderately between priors, with substantial overlap consistent with adequate data information for these two parameters. In contrast, λ exhibits marked prior sensitivity: the mean increases from 3.994 (CrI [0.470, 13.550]) under $\mathcal{P}_0$ to 25.450 (CrI [2.412, 73.060]) under $\mathcal{P}_{\mathrm{WI}}$. Together with poor mixing, this indicates that the data under PC is relatively weakly informative about λ.

The trace plots for the unknown parameters and the posterior density function plots of the method α, β, λ, $S(t)$, and $h(t)$ at t=0.5 are presented in Figures 7–11, which provide a visual representation of the posterior distributions and the convergence behavior of the $MCMC$ samples for the specified parameters.

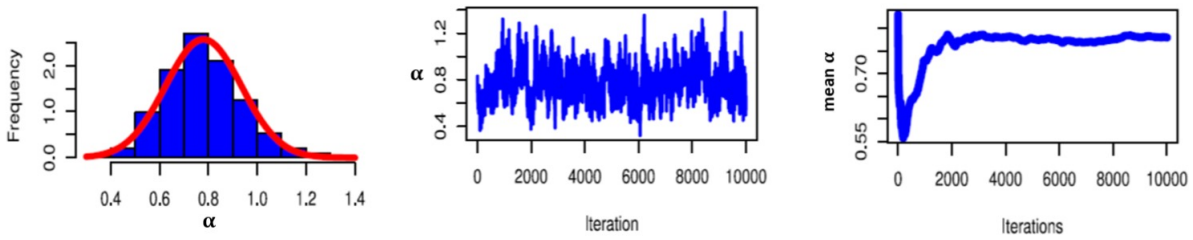

Figure 7. Distribution of posterior samples generated from MCMC with 10.000 iterations for the IPMC-J distribution with parameter α at $m = 10, n = 27$.

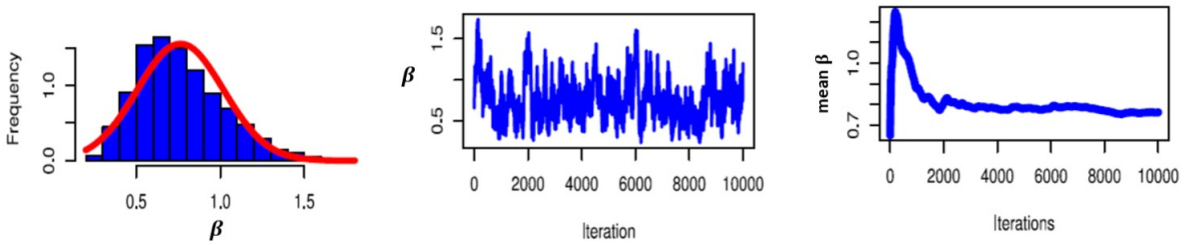

Figure 8. Distribution of posterior samples generated from MCMC with 10.000 iterations for the IPMC-J distribution with parameter β at $m = 10, n = 27$.

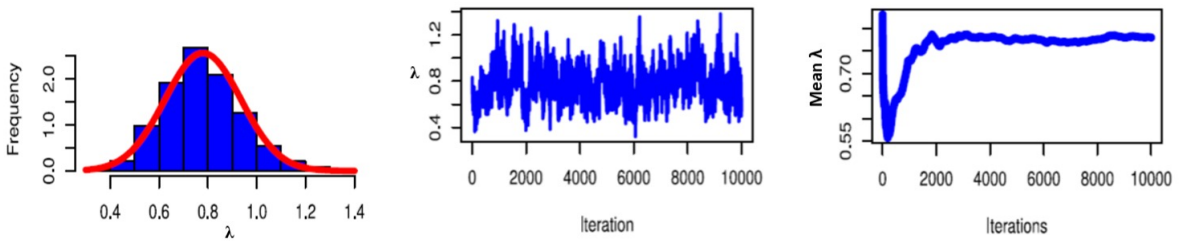

Figure 9. Distribution of posterior samples generated from MCMC with 10.000 iterations for the IPMC-J distribution for λ at $m = 10, n = 27$.

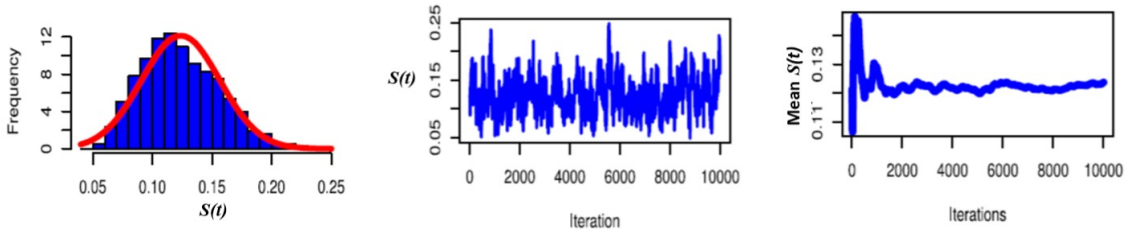

Figure 10. Distribution of posterior samples generated from MCMC with 10.000 iterations for the IPMC-J distribution for $S(y)$ at $m = 10, n = 27$.

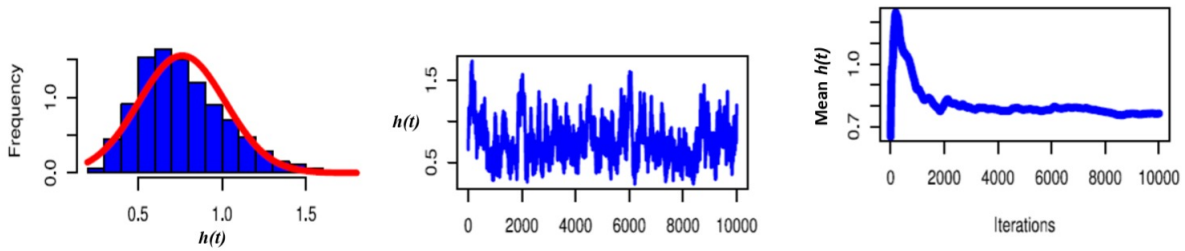

Figure 11. Distribution of posterior samples generated from MCMC with 10.000 iterations for the IPMC-J distribution for $h(y)$ at $m = 10, n = 27$.

7.3. Comparison with complete data

We compare model-fit criteria using the complete infant-mortality dataset. This exercise is especially informative for the small-sample case (the 2021 example), providing additional evidence for the suitability of the IPMCJ model and clarifying the performance gains achieved by progressive censoring relative to complete data. The results are summarized in Tables 14 and 15.

Table 14. The statistics of model selection criteria for the distributions fitted to infant mortality data with complete sample data ($n = 27$).

Model	*-L*	*AIC*	*BIC*	*CAIC*	W*	A*	*K–S*	*P*-value
IPMC-J(α, β, λ)	102.66	207.33	208.62	207.49	0.047	0.30	0.11	0.8477
TPCJ(β, λ)	106.16	216.31	218.90	216.81	0.11	0.75	0.16	0.5345
Burr III(β, λ)	119.08	242.16	244.75	242.66	0.04	0.26	0.36	0.0021
EIE(β, λ)	103.88	211.76	214.36	212.26	0.08	0.50	0.17	0.4187
Weibull (β, λ)	106.11	231.36	233.95	231.86	0.13	0.82	0.32	0.0084
Gamma(β, λ)	105.76	217.90	220.49	218.40	0.13	0.82	0.18	0.3436
Lomax(β, λ)	106.17	216.33	218.92	216.83	0.11	0.71	0.16	0.5158
C-J(β)	112.39	226.77	228.07	226.93	0.17	1.10	0.28	0.0260

Table 15. Comparison of IPMCJ model fit under PC vs. Complete Data with $n = 27$.

Criterion	Progressive Censoring (PC)	Complete Data
Log-likelihood ($-L$)	**99.66**	102.66
AIC	**201.33**	207.33
BIC	**201.62**	208.62
CAIC	**201.49**	207.49
W^*	**0.037**	0.047
A^*	**0.20**	0.30
K–S Statistic	**0.04**	0.11
P-value	0.645	**0.8477**

A comparison between the PC scheme and the complete data scenario is explored in Table 15, specifically highlighting the IPMCJ model performance across key metrics.

From Tables 14 and 15 the following results can be noticed:

a) Under the PC scheme, the log-likelihood is slightly lower (99.66 vs. 102.66), indicating a better fit.

b) The AIC, BIC, and CAIC values are all lower under PC, providing stronger evidence for the superiority of the IPMCJ model when fitted to censored data.

c) The error metrics W^* and A^* are also clearly improved under PC, demonstrating more accurate model performance. The Kolmogorov-Smirnov (K-S) statistic is smaller under PC (0.04 vs. 0.11), suggesting a closer empirical fit to the observed data.

d) Although the P-value is slightly higher in the complete data case, it remains well above the threshold under PC ($0.645 > 0.05$), thus supporting the adequacy of the model even in the presence of censoring.

When comparing all models in both settings, it is clear that the PC scheme has lower metrics when compared to the complete case. These findings indicate that PC allows for a more efficient and reliable estimation process without compromising model accuracy. Furthermore, the superior performance of the IPMCJ model under both schemes reassures its robustness and suitability for infant mortality analysis under incomplete data settings.

7.4. Comparison with nonparametric survival analysis

To further validate the performance of the proposed IPMCJ distribution, we conducted a comparison with the nonparametric KM estimator, which serves as a benchmark in survival analysis. The KM method was applied to the same progressively censored infant mortality dataset used in Section 6.1. The initial values of (α, β, λ) were selected using MLEs. These values provided stable starting points for optimization routines. In Bayesian analysis, different sets of initial values were tested, and all chains converged to the same posterior distribution, indicating robustness with respect to initialization.

Assuming ($\alpha = 0.4584, \beta = 1.7431, \lambda = 9.7349$), which were selected based on the best values with the minimum error attained, we computed the survival function of the IPMCJ distribution and compared it to the KM estimate. Figure 12 shows the resulting survival curves, while Table 16 provides a point-wise comparison of survival probabilities.

To assess the accuracy of the parametric model, we computed the following metrics:

- The integrated absolute error (IAE), which quantifies the total absolute deviation between the two survival curves.
- The MSE, which penalizes larger deviations and highlights overall fit quality.

The numerical results are as follows: IAE = 0.1, and MSE = 0.001. These findings demonstrate that the IPMCJ model closely approximates the nonparametric KM survival function across the time domain. The small error values and consistent behavior of the parametric model confirm its effectiveness in modeling censored infant mortality data.

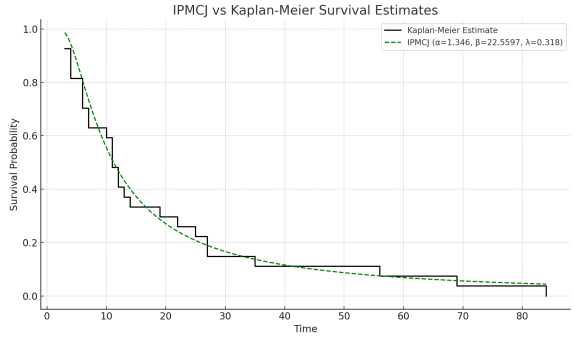

Figure 12. Comparison of KM estimate and IPMCJ survival function.

Table 16. Pointwise comparison of KM and IPMCJ survival probabilities.

Time (t)	KM Survival	IPMCJ Survival	Abs Error
3.00	0.963	0.961	0.0016
3.41	0.932	0.930	0.0015
3.81	0.900	0.899	0.0015
4.22	0.877	0.875	0.0014
4.62	0.861	0.859	0.0014

8. Simulation data

The MCMC procedure was run for 10,000 iterations, discarding the initial 2,000 burn-in iterations as a burn-in period. *Mathematics 13* was used for generating samples from the PC scheme to evaluate the parameter estimation methods in addition to the hazard and reliability functions of the IPMCJ. The starting initial values of $\alpha_0 = 1.5$, $\beta_0 = 0.9$ and $\lambda_0 = 0.6$ are predetermined. The MSE of the estimators corresponding to the parameters obtained for α, β, λ, $S(y)$, and $h(y)$, as $y = 0.5$ was computed by comparing the results from various methods.

Additionally, the 95% CI estimations are derived using the asymptotic distributions of the MLE and CRI. To evaluate the effectiveness of the estimation methods studied, the (CP) and the (ACL) are calculated.

In this research, the following PC schemes are considered:

Scheme I: $R_1 = n - m$, $R_i = 0$ for $i \neq 1$.

Scheme II: $R_{\frac{m}{2}} = R_{\frac{m}{2}+1} = \frac{n-m}{2}, R_i = 0$ for $i \neq \frac{m}{2}$ *and* $i \neq \frac{m}{2} + 1$.

Scheme III : $R_m = n - m$, $R_i = 0$ for $i \neq m$.

Tables 17–21 present the estimated parameters and the survival function along with their MSE, while Tables 22 and 23 display the outcomes of ACL and CP for the 95% CI. From the results, the following observations can be made:

(1) As the sample size increases, the MSE decrease, with the Bayesian estimation exhibiting the smallest MSE for α, β, $\lambda, S(y)$ and $h(y)$. Consequently, the performance of the Bayesian estimation outperforms the MLE in all the scenarios examined.

(2) In the sense that MSE are smaller, Bayesian estimation under LINEX with $c = -2$ better results estimates.

(3) In terms of smaller MSE, the Bayesian estimation under the LINEX loss function with $c = -2$ provides better results for the estimates.

(4) Scheme I outperforms Schemes II and III in terms of MSE when the sample size n and the effective size m are fixed.

(5) As shown in Tables 22 and 23, it can be seen that *CRI* provides more accurate results. Furthermore, ACI is evaluated for different sample sizes, observed failures, and schemes.

Table 17. The MLE and Bayesian estimates of α ($\alpha_0 = 1.5$) with (MSE) under various censoring schemes.

(n, m)	CS	MLE	SEL	LINEX (c)		
				−2	0.0001	2
(15,10)	I	1.2054	1.2054	1.2055	1.2054	1.2053
		(1.6875)	(1.6875)	(1.2055)	(1.6875)	(1.6874)
	II	1.1505	1.1505	1.1510	1.1505	1.1500
		(1.6260)	(1.6260)	(1.6278)	(1.6260)	(1.6243)
	III	1.3062	1.3062	1.3062	1.3062	1.3062
		(2.0331)	(2.0331)	(2.0333)	(2.0329)	(2.0331)
(20,15)	I	1.0948	1.0911	1.0913	1.0910	1.0911
		(1.3633)	(1.3609)	(1.3610)	(1.3608)	(1.3609)
	II	1.1097	1.1101	1.1101	1.1101	1.1101
		(1.7258)	(1.7277)	(1.7278)	(1.7277)	(1.7277)
	III	1.2105	1.2099	1.2100	1.2097	1.2099
		(1.7423)	(1.7418)	(1.7419)	(1.7416)	(1.7418)
(30,20)	I	1.0595	1.0593	1.0593	1.0593	1.0593
		(1.1058)	(1.1064)	(1.1064)	(1.1064)	(1.1064)
	II	1.1987	1.1987	1.1987	1.1987	1.1987
		(1.7477)	(1.7501)	(1.7502)	(1.7501)	(1.7501)
	III	1.3063	1.3052	1.3052	1.3052	1.3052
		(1.9163)	(1.9111)	(1.9111)	(1.9111)	(1.9111)
(40,20)	I	1.0471	1.0471	1.0471	1.0471	1.0471
		(1.2423)	(1.2427)	(1.2427)	(1.2427)	(1.2427)
	II	0.8983	0.8985	0.8985	0.8985	0.8985
		(0.9191)	(0.9186)	(0.9186)	(0.9185)	(0.9186)
	III	1.1884	1.1885	1.1885	1.1885	1.1885
		(1.6887)	(1.6879)	(1.6880)	(1.6879)	(1.6879)
(50,20)	I	1.0022	1.0027	1.0027	1.0027	1.0027
		(1.0548)	(1.0553)	(1.0553)	(1.0553)	(1.0553)
	II	1.0900	1.0900	1.0900	1.0900	1.0900
		(1.4578)	(1.4552)	(1.4554)	(1.4551)	(1.4552)
	III	0.9891	0.9889	0.9889	0.9889	0.9889
		(1.4338)	(1.4298)	(1.4299)	(1.4297)	(1.4298)

Table 18. MSE of MLE and Bayesian estimates of β ($\beta_0 = 0.9$) under various censoring schemes.

(n, m)	CS	MLE	SEL	LINEX (c)		
				−2	0.0001	2
(15,10)	I	1.1629	1.1632	1.1635	1.1632	1.1635
		(1.0444)	(1.0445)	(1.0450)	(1.0445)	(1.0442)
	II	1.0970	1.0961	1.0965	1.0961	1.0965
		(0.9978)	(0.9977)	(0.9982)	(0.9977)	(0.9973)
	III	1.2388	1.2383	1.2384	1.2383	1.2384
		(1.3310)	(1.3300)	(1.3301)	(1.3300)	(1.3299)
(20,15)	I	1.0629	1.0668	1.0670	1.0668	1.0670
		(0.8555)	(0.8642)	(0.8647)	(0.8642)	(0.8638)
	II	1.0636	1.0634	1.0634	1.0634	1.0634
		(0.9187)	(0.9195)	(0.9195)	(0.9195)	(0.9195)
	III	1.1837	1.1777	1.1778	1.1777	1.1778
		(1.1055)	(1.1007)	(1.1007)	(1.1007)	(1.1007)
(30,20)	I	1.1282	1.1277	1.1277	1.1277	1.1277
		(0.9462)	(0.9455)	(0.9455)	(0.9455)	(0.9455)
	II	1.1784	1.1785	1.1785	1.1785	1.1785
		(1.1129)	(1.1125)	(1.1125)	(1.1125)	(1.1125)
	III	1.2268	1.2278	1.2278	1.2278	1.2278
		(1.2284)	(1.2311)	(1.2311)	(1.2311)	(1.2311)
(40,20)	I	1.0557	1.0553	1.0553	1.0553	1.0553
		(0.8785)	(0.8773)	(0.8773)	(0.8773)	(0.8773)
	II	0.9373	0.9373	0.9373	0.9373	0.9373
		(0.7651)	(0.7649)	(0.7649)	(0.7648)	(0.7649)
	III	1.1363	1.1358	1.1358	1.1358	1.1358
		(1.2943)	(1.2936)	(1.2937)	(1.2936)	(1.2936)
(50,20)	I	1.0408	1.0402	1.0402	1.0402	1.0402
		(0.8426)	(0.8418)	(0.8418)	(0.8418)	(0.8418)
	II	1.0900	1.0801	1.0801	1.0801	1.0801
		(0.8998)	(0.9006)	(0.9006)	(0.9006)	(0.9006)
	III	0.8974	0.8967	0.8967	0.8967	0.8967
		(0.8951)	(0.8938)	(0.8938)	(0.8938)	(0.8938)

Table 19. MSE of MLE and Bayesian estimates of λ ($\lambda_0 = 0.6$) under various censoring schemes.

(n, m)	CS	MLE	SEL	LINEX (c)		
				−2	0.0001	2
(15,10)	I	0.6345	0.6345	0.6345	0.6345	0.6345
		(0.4353)	(0.4354)	(0.4354)	(0.4354)	(0.4354)
	II	0.7250	0.7246	0.7246	0.7246	0.7246
		(0.6278)	(0.6276)	(0.6276)	(0.6276)	(0.6276)
	III	0.8389	0.8389	0.8389	0.8389	0.8389
		(1.1412)	(1.1408)	(1.1408)	(1.1408)	(1.1408)
(20,15)	I	0.7283	0.7290	0.7290	0.7290	0.7290
		(0.7502)	(0.7510)	(0.7510)	(0.7510)	(0.7510)
	II	0.6847	0.6846	0.6846	0.6846	0.6846
		(0.4874)	(0.4873)	(0.4873)	(0.4873)	(0.4873)
	III	0.5895	0.5896	0.5896	0.5896	0.5896
		(0.2801)	(0.2801)	(0.2801)	(0.2801)	(0.2801)
(30,20)	I	0.6022	0.6022	0.6022	0.6022	0.6022
		(0.4629)	(0.4630)	(0.4630)	(0.4630)	(0.4630)
	II	0.5405	0.5405	0.5405	0.5405	0.5405
		(0.2094)	(0.2096)	(0.2096)	(0.2096)	(0.2096)
	III	0.5461	0.5460	0.5460	0.5460	0.5460
		(0.1868)	(0.1870)	(0.1870)	(0.1870)	(0.1870)
(40,20)	I	0.5891	0.5892	0.5892	0.5892	0.5892
		(0.3204)	(0.3200)	(0.3200)	(0.3200)	(0.3200)
	II	0.6785	0.6786	0.6786	0.6786	0.6786
		(0.3865)	(0.3868)	(0.3868)	(0.3868)	(0.3868)
	III	0.8301	0.8306	0.8306	0.8306	0.8306
		(1.0881)	(1.0921)	(1.0921)	(1.0921)	(1.0921)
(50,20)	I	0.5975	0.5974	0.5974	0.5974	0.5974
		(0.2298)	(0.2299)	(0.2299)	(0.2299)	(0.2299)
	II	0.5408	0.5409	0.5409	0.5409	0.5409
		(0.1396)	(0.1396)	(0.1396)	(0.1396)	(0.1396)
	III	1.0164	1.0165	1.0165	1.0165	1.0165
		(1.3524)	(1.3517)	(1.3518)	(1.3517)	(1.3517)

Table 20. MSE of MLE and Bayesian estimates of h ($h_0 = 0.5$) under various censoring schemes.

(n, m)	CS	MLE	SEL	LINEX (c)		
				−2	0.0001	2
(15,10)	I	0.3394	0.3394	0.3394	0.3394	0.3394
		(0.0243)	(0.0243)	(0.0243)	(0.0243)	(0.0243)
	II	0.3510	0.3516	0.3518	0.3516	0.3518
		(0.0346)	(0.0352)	(0.0354)	(0.0352)	(0.0350)
	III	0.3843	0.3840	0.3840	0.3840	0.3840
		(0.1493)	(0.1492)	(0.1492)	(0.1492)	(0.1492)
(20,15)	I	0.3443	0.3430	0.3430	0.3430	0.3430
		(0.0217)	(0.0215)	(0.0215)	(0.0215)	(0.0215)
	II	0.3225	0.3225	0.3225	0.3225	0.3225
		(0.0103)	(0.0103)	(0.0103)	(0.0103)	(0.0103)
	III	0.3273	0.3283	0.3283	0.3283	0.3283
		(0.0147)	(0.0149)	(0.0150)	(0.0149)	(0.0149)
(30,20)	I	0.3080	0.3080	0.3080	0.3080	0.3080
		(0.0098)	(0.0098)	(0.0098)	(0.0098)	(0.0098)
	II	0.3185	0.3183	0.3183	0.3183	0.3183
		(0.0097)	(0.0096)	(0.0096)	(0.0096)	(0.0096)
	III	0.3270	0.3266	0.3266	0.3266	0.3266
		(0.0119)	(0.0118)	(0.0118)	(0.0118)	(0.0118)
(40,20)	I	0.5891	0.5892	0.5892	0.5892	0.5892
		(0.3204)	(0.3200)	(0.3200)	(0.3200)	(0.3200)
	II	0.6785	0.6786	0.6786	0.6786	0.6786
		(0.3865)	(0.3868)	(0.3868)	(0.3868)	(0.3868)
	III	0.8301	0.8306	0.8306	0.8306	0.8306
		(1.0881)	(1.0921)	(1.0921)	(1.0921)	(1.0921)
(50,20)	I	0.5975	0.5974	0.5974	0.5974	0.5974
		(0.2298)	(0.2299)	(0.2299)	(0.2299)	(0.2299)
	II	0.5408	0.5409	0.5409	0.5409	0.5409
		(0.1396)	(0.1396)	(0.1396)	(0.1396)	(0.1396)
	III	1.0164	1.0165	1.0165	1.0165	1.0165
		(1.3524)	(1.3517)	(1.3517)	(1.3517)	(1.3517)

Table 21. MSE of MLE and Bayesian estimation of S ($S_0 = 0.5$).

(n, m)	CS	MLE	SEL	LINEX		
				$c = -2$	$c = 2$	$c = 0.0001$
(15,10)	I	0.6536	0.6536	0.6530	0.6537	0.6536
	II	0.6596	0.6588	0.6589	0.6589	0.6588
	III	0.6612	0.6614	0.6615	0.6615	0.6614
(20,15)	I	0.6515	0.6531	0.6531	0.6531	0.6531
	II	0.6677	0.6676	0.6676	0.6676	0.6676
	III	0.6639	0.6617	0.6618	0.6618	0.6617
(30,20)	I	0.6673	0.6672	0.6672	0.6672	0.6672
	II	0.6609	0.6610	0.6610	0.6610	0.6610
	III	0.6547	0.6551	0.6551	0.6551	0.6551
(40,20)	I	0.6600	0.6600	0.6600	0.6600	0.6600
	II	0.6667	0.6666	0.6666	0.6666	0.6666
	III	0.6616	0.6615	0.6615	0.6615	0.6615
(50,20)	I	0.6727	0.6722	0.6722	0.6722	0.6722
	II	0.6607	0.6606	0.6606	0.6606	0.6606
	III	0.6496	0.6493	0.6493	0.6493	0.6493

Table 22. ACL and CP of 95% CIs for the parameters α, β, and λ.

(n, m)	CS	α		β		λ	
		MLE	MCMC	MLE	MCMC	MLE	MCMC
(15,10)	I	15.9457 (0.9295)	0.0107 (0.9519)	14.3017 (0.9566)	0.0100 (0.9368)	70.3159 (0.9610)	0.0029 (0.9704)
	II	22.1548 (0.9316)	0.0133 (0.9321)	19.4649 (0.9713)	0.0109 (0.9628)	174.8970 (0.9588)	0.0033 (0.9724)
	III	19.7624 (0.9346)	0.0130 (0.9342)	13.9589 (0.9333)	0.0091 (0.9333)	29.3361 (0.9618)	0.0034 (0.9450)
(20,10)	I	18.9659 (0.9738)	0.0127 (0.9582)	17.3103 (0.9695)	0.0110 (0.9621)	52.7671 (0.9599)	0.0041 (0.9642)
	II	9.2913 (0.9557)	0.0054 (0.9618)	6.1725 (0.9370)	0.0041 (0.9437)	1.8451 (0.9567)	0.0017 (0.9695)
	III	19.8829 (0.9298)	0.0125 (0.9648)	16.5598 (0.9581)	0.0093 (0.9326)	0.9530 (0.9691)	0.0034 (0.9637)
(30,20)	I	7.8598 (0.9266)	0.0052 (0.9469)	6.4500 (0.9712)	0.0041 (0.9585)	3.7312 (0.9681)	0.0018 (0.9420)
	II	9.4316 (0.9487)	0.0059 (0.9578)	6.9406 (0.9655)	0.0044 (0.9552)	5.8039 (0.9453)	0.0015 (0.9451)
	III	15.1179 (0.9410)	0.0096 (0.9485)	9.5790 (0.9489)	0.0066 (0.9690)	2.4636 (0.9283)	0.0015 (0.9583)
(40,20)	I	7.0326 (0.9676)	0.0048 (0.9296)	5.2828 (0.9563)	0.0038 (0.9326)	1.6746 (0.9533)	0.0015 (0.9463)
	II	8.0517(0.9558)	0.0054(0.9749)	6.8454 (0.9745)	0.0047(0.9514)	2.4923 (0.9401)	0.0016(0.9500)
	III	13.1705 (0.9573)	0.0081 (0.9413)	8.2766 (0.9533)	0.0052 (0.9397)	10.9228(0.9536)	0.0023 (0.9555)
(50,20)	I	7.5517(0.9314)	0.0050 (0.9530)	6.1892(0.9486)	0.0044 (0.9448)	5.7893 (0.9378)	0.0016(0.9273)
	II	9.7014(0.9480)	0.0071(0.9392)	7.6457(0.9415)	0.0053(0.9696)	4.0445 (0.9506)	0.0017 (0.9493)
	III	11.2246 (0.9443)	0.0076 (0.9698)	7.7455(0.9647)	0.0046(0.9556)	39.0536(0.9312)	0.0043 (0.9702)

Table 23. ACL and CP of 95% credible intervals for $S(y)$ and $h(y)$.

(n,m)	CS	$S(y)$		$h(y)$	
		MLE	MCMC	MLE	MCMC
(15,10)	I	0.9105 (0.9642)	0.0039 (0.9378)	1.0109 (0.9617)	0.0034 (0.9336)
	II	0.5774 (0.9341)	0.0046 (0.9309)	0.8381 (0.9363)	0.0053 (0.9634)
	III	0.4575 (0.9731)	0.0035 (0.9410)	0.6963 (0.9617)	0.0034 (0.9590)
(20,10)	I	0.5406 (0.9696)	0.0038 (0.9306)	0.6972 (0.9413)	0.0049 (0.9387)
	II	0.3553 (0.9583)	0.0016 (0.9424)	0.3926 (0.9595)	0.0014 (0.9507)
	III	0.4786 (0.9350)	0.0045 (0.9665)	0.4591 (0.9736)	0.0044 (0.9280)
(30,20)	I	0.3637 (0.9390)	0.0018 (0.9321)	0.3597 (0.9352)	0.0018 (0.9295)
	II	0.3145 (0.9640)	0.0019 (0.9365)	0.3632 (0.9554)	0.0017 (0.9718)
	III	0.2981 (0.9289)	0.0024 (0.9393)	0.3426 (0.9591)	0.0022 (0.9622)
(40,20)	I	0.3284 (0.9379)	0.0015 (0.9382)	0.3300 (0.9506)	0.0014 (0.9398)
	II	0.2809 (0.9666)	0.0020 (0.9658)	0.3791 (0.9515)	0.0018 (0.9507)
	III	0.2670 (0.9279)	0.0021 (0.9280)	0.4842 (0.9531)	0.0019 (0.9346)
(50,20)	I	0.3396 (0.9467)	0.0019 (0.9581)	0.3631 (0.9453)	0.0018 (0.9392)
	II	0.2760 (0.9283)	0.0021 (0.9317)	0.4500 (0.9334)	0.0021 (0.9360)
	III	0.2655 (0.9632)	0.0023 (0.9390)	0.7756 (0.9713)	0.0021 (0.9649)

9. Conclusions

In this study, both classical and Bayesian estimation methods were employed to estimate the parameters of the IPMCJ distribution under a progressive censoring scheme. The MLE method was used to obtain point and interval estimates, while the Bayesian estimation approach was developed under two types of priors: non-informative and informative, to assess the sensitivity of inference to prior information. Due to the analytical complexity of the posterior distributions, the MCMC technique, combined with the M-H algorithm, was implemented to compute the Bayesian estimates and corresponding credible intervals. Diagnostic tests, including maximum likelihood check and convergence assessment with posterior trace plots, were performed to confirm the accuracy and stability of the MLE and the Bayesian inference.

A nonparametric comparison using the KM estimator was also conducted to validate the flexibility and goodness-of-fit of the proposed IPMCJ distribution. The IPMCJ model showed excellent agreement with the nonparametric KM curve, demonstrating its effectiveness in modeling real-life data. The simulation results further revealed that Bayesian estimation under the LINEX loss function outperformed the classical MLE and bootstrap approaches by producing more stable and valid parameter estimates, especially under censoring.

These results highlight the advantages of combining MLE and Bayesian inference with diagnostic analysis and prior sensitivity assessment. The proposed IPMCJ framework thus provides a powerful and flexible tool for modeling incomplete lifetime data, offering both theoretical and practical reliability for medical and industrial applications.

Future studies can extend this work by considering different lifetime models, in addition to selecting

different priors to assess the sensitivity of Bayesian estimation. Different censoring schemes, such as adaptive, hybrid, or joint progressive censoring, can also be explored. Moreover, further diagnostic tests for MCMC convergence and model comparison criteria may be included to strengthen the Bayesian results. Applying the IPMCJ model to larger medical and industrial datasets would help confirm its reliability and practical usefulness.

Author contributions

M.Y.A.: Conceptualization, Methodology, Validation, Resources, Writing–original draft preparation; D.A.R.: Conceptualization, Methodology, Software, Formal analysis, Data curation, Writing–review & editing, Supervision, Project administration; H.H.A.: Software, Validation, Formal analysis, Investigation, Data curation, Writing–review & editing, Visualization, Project administration, Funding acquisition; B.S.E.-D.: Conceptualization, Methodology, Formal analysis, Investigation, Supervision. All authors have read and agreed to the published version of the manuscript.

Use of Generative-AI tools declaration

The authors declare they have not used Artificial Intelligence (AI) tools in the creation of this article.

Funding

This work was supported by the Deanship of Scientific Research, Vice Presidency for Graduate Studies and Scientific Research, King Faisal University, Saudi Arabia [GRANT No. KFU253633].

Conflict of interest

The authors declare no conflict of interest.

Data Availability

A description of the infant mortality rate per 1000 live births for several selected countries in 2021 and 2023 as reported by the World Bank (`https://data.worldbank.org/indicator/SP.DYN.IMRT.IN`) is included to support the findings of this study.

References

1. A. C. Cohen, Progressively censored samples in life testing, *Technometrics*, **5** (1963), 327–339. https://doi.org/10.2307/1266337
2. N. Balakrishnan, R. A. Sandhu, A simple simulation algorithm for generating progressive type-II censored samples, *Amer. Stat.*, **49** (1995), 229–230. https://doi.org/10.1080/00031305.1995.10476150
3. N. Balakrishnan, R. Aggarwala, *Progressive censoring: theory, methods, and applications*, Boston: Birkhäuser, 2000. https://doi.org/10.1007/978-1-4612-1334-5

4. N. Balakrishnan, E. Cramer, *The art of progressive censoring: applications to reliability and quality*, New York: Birkhäuser, 2014. https://doi.org/10.1007/978-0-8176-4807-7

5. D. Kundu, Bayesian inference and life testing plan for the Weibull distribution in presence of progressive censoring, *Technometrics*, **50** (2008), 144–154. https://doi.org/10.1198/004017008000000217

6. S. K. Ashour, A. A. El-Sheikh, A. Elshahhat, Inferences and optimal censoring schemes for progressively first-failure censored Nadarajah-Haghighi distribution, *Sankhya A*, **84** (2020), 885–923. https://doi.org/10.1007/s13171-019-00175-2

7. N. Feroze, M. Noor-ul-Amin, M. Sadiq, M. M. Hossain, On optimal progressive censoring schemes from models with U-shaped hazard rate: a comparison between conventional and fuzzy priors, *J. Funct. Space.*, **2022** (2022), 2336760. https://doi.org/10.1155/2022/2336760

8. B. Laumen, E. Cramer, Progressive censoring with fixed censoring times, *Statistics*, **53** (2019), 569–600. https://doi.org/10.1080/02331888.2019.1579817

9. E. Cramer, J. Navarro, The progressive censoring signature of coherent systems, *Appl. Stoch. Model. Bus. Ind.*, **32** (2016), 697–710. https://doi.org/10.1002/asmb.2188

10. E. A. Ahmed, Estimation of some lifetime parameters of generalized Gompertz distribution under progressively type-II censored data, *Appl. Math. Model.*, **39** (2015), 5567–5578. https://doi.org/10.1016/j.apm.2015.01.023

11. E. M. Almetwally, H. M. Almongy, A. El Sayed Mubarak, Bayesian and maximum likelihood estimation for the Weibull generalized exponential distribution parameters using progressive censoring schemes, *Pak. J. Stat. Oper. Res.*, **14** (2018), 853–868. https://doi.org/10.18187/pjsor.v14i4.2600

12. H. Haj Ahmad, Best prediction method for progressive type-II censored samples under new Pareto model with applications, *J. Math.*, **2021** (2021), 1355990. https://doi.org/10.1155/2021/1355990

13. H. Haj Ahmad, E. Elnagar, D. Ramadan, Investigating the lifetime performance index under Ishita distribution based on progressive type II censored data with applications, *Symmetry*, **15** (2023), 1779. https://doi.org/10.3390/sym15091779

14. C. I. Ezeilo, O. S. I., E. U. Umeh, C. K. Onyekwere, On power Chris-Jerry distribution: properties and parameter estimation methods, *Asian Journal of Probability and Statistics*, **25** (2023), 29–44. https://doi.org/10.9734/ajpas/2023/v25i3562

15. M. Y. Awajan, D. A. Ramadan, B. S. El-Desouky, Inverse power modified Chris-Jerry distribution: properties, estimation, simulation and medical application, *Appl. Math. Inf. Sci.*, **18** (2024), 1261–1271. https://doi.org/10.18576/amis/180608

16. S. K. Tse, C. Yang, H.-K. Yuen, Statistical analysis of Weibull distributed lifetime data under type II progressive censoring with binomial removals, *J. Appl. Stat.*, **27** (2000), 1033–1043. https://doi.org/10.1080/02664760050173355

17. R. Aggarwala, N. Balakrishnan, Some properties of progressive censored order statistics from arbitrary and uniform distributions with applications to inference and simulation, *J. Stat. Plan. Infer.*, **70** (1998), 35–49. https://doi.org/10.1016/S0378-3758(97)00173-0

18. U. H. Salemi, S. Rezaei, S. Nadarajah, A-optimal and D-optimal censoring plans in progressively type-II right censored order statistics, *Stat. Papers*, **60** (2019), 1349–1367. https://doi.org/10.1007/s00362-017-0877-9
19. X. Qin, J. Yu, W. Gui, Goodness-of-fit test for exponentiality based on spacings for general progressive type-II censored data, *J. Appl. Stat.*, **49** (2022), 599–620. https://doi.org/10.1080/02664763.2020.1821613
20. K. Maiti, S. Kayal, Estimation of parameters and reliability characteristics for a generalized Rayleigh distribution under progressive type-II censored sample, *Commun. Stat.-Simul. Comput.*, **50** (2021), 3669–3698. https://doi.org/10.1080/03610918.2019.1630431
21. H. Haj Ahmad, D. A. Ramadan, Investigating risk factors under progressive type-II censoring scheme: statistical inference and modeling, *AIP Conf. Proc.*, **3301** (2025), 050009. https://doi.org/10.1063/5.0262301
22. E. H. Khalifa, D. A. Ramadan, H. N. Alqifari, B. S. El-Desouky, Bayesian inference for inverse power exponentiated Pareto distribution using progressive type-II censoring with application to flood-level data analysis, *Symmetry*, **16** (2024), 309. https://doi.org/10.3390/sym16030309
23. V. K. Sharma, S. K. Singh, U. Singh, V. Agiwal, The inverse Lindley distribution: a stress-strength reliability model with application to head and neck cancer data, *J. Ind. Prod. Eng.*, **32** (2015), 162–173. https://doi.org/10.1080/21681015.2015.1025901
24. M. S. Khan, G. R. Pasha, A. H. Pasha, Theoretical analysis of inverse Weibull distribution, *WSEAS Transactions on Mathematics*, **2** (2008), 30–38.
25. D. Kundu, H. Howlader, Bayesian inference and prediction of the inverse Weibull distribution for Type-II censored data, *Comput. Stat. Data Anal.*, **54** (2010), 1547–1558. https://doi.org/10.1016/j.csda.2010.01.003
26. K. A. Elnagar, D. A. Ramadan, B. S. El-Desouky, Statistical inference to the parameter of the inverse power Ishita distribution under progressive type II censored data with application to COVID-19 data, *J. Math.*, **2022** (2022), 7704167. https://doi.org/10.1155/2022/7704167
27. H. S. Jabarah, A. H. Tolba, A. T. Ramadan, A. I. El-Gohary, The truncated unit Chris-Jerry distribution and its applications, *Appl. Math. Inf. Sci.*, **18** (2024), 1317–1330. https://doi.org/10.18576/amis/180613
28. J. F. Lawless, *Statistical models and methods for lifetime data*, 2 Eds., Wiley, 2011.
29. W. H. Greene, *Econometric analysis*, 5 Eds., India: Pearson Education, 2003.
30. P. Hall, Theoretical comparison of bootstrap confidence intervals, *Ann. Stat.*, **16** (1988), 927–953. https://doi.org/10.1214/aos/1176350933
31. S. J. Press, *Subjective and objective Bayesian statistics: principles, models, and applications*, 2 Eds., Wiley, 2009.
32. H. R. Varian, A Bayesian approach to real estate assessment, In: *Studies in Bayesian econometrics and statistics: in honor of Leonard J. Savage*, North-Holland, 1975, 195–208.
33. N. Metropolis, A. W. Rosenbluth, M. N. Rosenbluth, A. H. Teller, E. Teller, Equation of state calculations by fast computing machines, *J. Chem. Phys.*, **21** (1953), 1087–1092. https://doi.org/10.1063/1.1699114

34. W. K. Hastings, Monte Carlo sampling methods using Markov chains and their applications, *Biometrika*, **57** (1970), 97–109. https://doi.org/10.1093/biomet/57.1.97

35. H. Haj Ahmad, D. A. Ramadan, E. M. Almetwally, Tampered random variable analysis in step-stress testing: modeling, inference, and applications, *Mathematics*, **12** (2024), 1248. https://doi.org/10.3390/math12081248

36. L. Tierney, Markov chains for exploring posterior distributions, *Ann. Stat.*, **22** (1994), 1701–1728. https://doi.org/10.1214/aos/1176325750

37. G. S. Mudholkar, D. K. Srivastava, Exponentiated Weibull family for analyzing bathtub failure-rate data, *IEEE Trans. Reliab.*, **42** (1993), 299–302. https://doi.org/10.1109/24.229504

38. T. Zhang, M. Xie, Failure data analysis with extended Weibull distribution, *Commun. Stat.-Simul. Comput.*, **36** (2007), 579–592. https://doi.org/10.1080/03610910701236081

39. E. W. Stacy, A generalization of the gamma distribution, *Ann. Math. Stat.*, **33** (1962), 1187–1192. https://doi.org/10.1214/aoms/1177704481

40. P. E. Oguntunde, A. O. Adejumo, E. A. Owoloko, On the exponentiated generalized inverse exponential distribution, In: *Proceedings of the world congress on engineering*, WCE 2017, July 5–7, 2017, London, 1–4.

41. C. D. Lai, M. Xie, D. N. P. Murthy, A modified Weibull distribution, *IEEE Trans. Reliab.*, **52** (2003), 33–37. https://doi.org/10.1109/TR.2002.805788

42. A. S. Papadopoulos, The Burr distribution as a failure model from a Bayesian approach, *IEEE Trans. Reliab.*, **27** (1978), 369–371. https://doi.org/10.1109/TR.1978.5220427

43. H. C. S. Thom, A note on the gamma distribution, *Mon. Weather Rev.*, **86** (1958), 117–122. https://doi.org/10.1175/1520-0493(1958)086¡0117:ANOTGD¿2.0.CO;2

44. C. K. Onyekwere, O. J. Obulezi, Chris-Jerry distribution and its applications, *Asian Journal of Probability and Statistics*, **20** (2022), 16–30. https://doi.org/10.9734/ajpas/2022/v20i130480

45. E. Q. Chinedu, Q. C. Chukwudum, N. Alsadat, O. J. Obulezi, E. M. Almetwally, A. H. Tolba, New lifetime distribution with applications to single acceptance sampling plan and scenarios of increasing hazard rates, *Symmetry*, **15** (2023), 1881. https://doi.org/10.3390/sym15101881

46. A. J. Lemonte, G. M. Cordeiro, An extended Lomax distribution, *Statistics*, **47** (2013), 800–816. https://doi.org/10.1080/02331888.2011.568119

Appendix A

$$E_i := \exp(y_i^{-\alpha}\beta),$$
$$\mathcal{D}_i := \left(2y_i^{\alpha}\beta + \beta^2 - (-1 + E_i)\, y_i^{2\alpha}(2 + \beta\lambda)\right)^2.$$

$$\frac{\partial^2 \ln L}{\partial \alpha^2} = -\frac{m}{\alpha^2} - 2\sum_{i=1}^{m} \frac{\beta\, y_i^{-2\alpha} (\ln y_i)^2 \left(2y_i^{-2\alpha} - \lambda - \beta y_i^{-2\alpha}\right)}{\left(\lambda + \beta y_i^{-2\alpha}\right)^2} - \sum_{i=1}^{m} R_i \, \frac{y_i^{\alpha}\, \beta^2\, \mathcal{N}_i\, (\ln y_i)^2}{\mathcal{D}_i},$$

$$\mathcal{N}_i = \beta^3 - (-1+E_i)\,y_i^{4\alpha}\,\lambda\,(2+\beta\lambda) + E_i\,y_i^{3\alpha}\,\beta\lambda\,(2+\beta\lambda) + y_i^{\alpha}\,\beta^2(4+E_i(2+\beta\lambda)) - y_i^{2\alpha}\,\beta(3E_i(2+\beta\lambda) - 2(3+\beta\lambda)).$$

$$\frac{\partial^2 \ln L}{\partial\alpha\,\partial\beta} = \sum_{i=1}^{m} y_i^{-\alpha}\,\ln y_i - 2\sum_{i=1}^{m}\frac{\lambda\,y_i^{-2\alpha}\,\ln y_i}{(\lambda+\beta y_i^{-2\alpha})^2} + \sum_{i=1}^{m} R_i\,\frac{y_i^{-\alpha}\,\beta\,\mathcal{M}_i\,\ln y_i}{\mathcal{D}_i},$$

$$\mathcal{M}_i = \beta^3 - 2(-1+E_i)\,y_i^{2\alpha}\,\beta\,(3+\beta\lambda) - (-1+E_i)\,y_i^{4\alpha}\,\lambda\,(4+\beta\lambda) + y_i^{3\alpha}\,\beta\lambda(2+E_i(2+\beta\lambda)) + y_i^{\alpha}\,\beta^2(4+E_i(2+\beta\lambda)).$$

$$\frac{\partial^2 \ln L}{\partial\alpha\,\partial\lambda} = \sum_{i=1}^{m}\frac{\beta\,y_i^{-2\alpha}\,\ln y_i}{(\lambda+\beta y_i^{-2\alpha})^2} - \sum_{i=1}^{m} R_i\,\frac{y_i^{\alpha}\,\beta^2\,(2(-1+E_i)\,y_i^{2\alpha} - 2y_i^{\alpha}\beta - E_i\beta^2)\,\ln y_i}{\mathcal{D}_i}.$$

$$\frac{\partial^2 \ln L}{\partial\beta^2} = -\frac{2m}{\beta^2} + \frac{m\lambda^2}{(\beta\lambda+2)^2} - \sum_{i=1}^{m}\frac{y_i^{-2\alpha}}{(\lambda+\beta y_i^{-2\alpha})^2} + \sum_{i=1}^{m} R_i\,\frac{\mathcal{B}_i}{(2+\beta\lambda)^2\,\mathcal{D}_i},$$

$$\mathcal{B}_i = 8(-1+E_i)\,y_i^{3\alpha}\,\lambda\,(2+\beta\lambda) + 4y_i^{\alpha}\beta\Big(-4(1+\beta\lambda) + E_i(2+\beta\lambda)^2\Big) - \beta^2\Big(8+8\beta\lambda+\beta^2\lambda^2 + E_i(2+\beta\lambda)^3\Big) - y_i^{2\alpha}\beta\lambda\Big(8+E_i(8+16\beta\lambda+8\beta^2\lambda^2+\beta^3\lambda^3)\Big).$$

$$\frac{\partial^2 \ln L}{\partial\beta\,\partial\lambda} = -\frac{2m}{(\beta\lambda+2)^2} - \sum_{i=1}^{m}\frac{y_i^{-2\alpha}}{(\lambda+\beta y_i^{-2\alpha})^2} - \sum_{i=1}^{m} R_i\,\frac{\beta\,C_i}{(2+\beta\lambda)^2\,\mathcal{D}_i},$$

$$C_i = 2\beta^3 - 8(-1+E_i)\,y_i^{3\alpha}\,(2+\beta\lambda) + y_i^{\alpha}\beta^2\Big(8+E_i(2+\beta\lambda)^2\Big) + y_i^{2\alpha}\beta\Big(20+8\beta\lambda+\beta^2\lambda^2 + E_i(-4+\beta^2\lambda^2)\Big).$$

$$\frac{\partial^2 \ln L}{\partial\lambda^2} = \frac{m\beta^2}{(\beta\lambda+2)^2} - \sum_{i=1}^{m}(\lambda+\beta y_i^{-2\alpha})^2 + \sum_{i=1}^{m} R_i\,\frac{\beta^3(2y_i^{\alpha}+\beta)(2y_i^{\alpha}\beta+\beta^2-2(-1+E_i)\,y_i^{2\alpha}(2+\beta\lambda))}{(2+\beta\lambda)^2\,\mathcal{D}_i}.$$

Appendix B

Algorithm 1: Newton–Raphson Algorithm

Input: Initial parameter vector $\theta^{(0)}$, tolerance ε, maximum iterations M
Output: Estimated parameter vector θ^*
Set $k = 0$;
while $k < M$ **do**
  Compute the log-likelihood $L(\theta^{(k)})$;
  Evaluate the score vector $U(\theta^{(k)}) = \frac{\partial L}{\partial \theta}$;
  Evaluate the observed information matrix $I(\theta^{(k)}) = -\frac{\partial^2 L}{\partial \theta^2}$;
  Update parameters: $\theta^{(k+1)} = \theta^{(k)} + [I(\theta^{(k)})]^{-1}U(\theta^{(k)})$;
  if $\|\theta^{(k+1)} - \theta^{(k)}\| < \varepsilon$ **then**
    Stop and set $\theta^* = \theta^{(k+1)}$
  Set $k = k + 1$;

Pseudo-code for MCMC via M–H

Algorithm 2: Metropolis–Hastings Algorithm

Input: Prior distribution $\pi(\theta)$, likelihood $L(\theta|\text{data})$, proposal $q(\theta'|\theta)$, initial value $\theta^{(0)}$, number of iterations N

Output: Posterior samples $\{\theta^{(1)}, \theta^{(2)}, \ldots, \theta^{(N)}\}$

Set $k = 0$;

for $t = 1$ **to** N **do**

Propose $\theta^* \sim q(\theta^*|\theta^{(t-1)})$;

Compute acceptance ratio:

$$\alpha = \min\left\{1, \frac{L(\theta^*|\text{data})\,\pi(\theta^*)\,q(\theta^{(t-1)}|\theta^*)}{L(\theta^{(t-1)}|\text{data})\,\pi(\theta^{(t-1)})\,q(\theta^*|\theta^{(t-1)})}\right\}$$

;

Generate $u \sim U(0, 1)$;

if $u \leq \alpha$ **then**

Accept θ^* and set $\theta^{(t)} = \theta^*$;

else

Reject θ^* and set $\theta^{(t)} = \theta^{(t-1)}$;

Discard burn-in samples and return the posterior sample set ;